HHS Public Access

Author manuscript

Prog Retin Eye Res. Author manuscript; available in PMC 2018 September 01.

Published in final edited form as:

Prog Retin Eye Res. 2017 September ; 60: 181–200. doi:10.1016/j.preteyeres.2017.04.001.

The Lens Growth Process

Steven Bassnett[a,*] and **Hrvoje Šikić**[b]

[a]Department of Ophthalmology & Visual Sciences, Washington University School of Medicine

[b]Department of Mathematics, Faculty of Science, University of Zagreb

Abstract

The factors that regulate the size of organs to ensure that they fit within an organism are not well understood. A simple organ, the ocular lens serves as a useful model with which to tackle this problem. In many systems, considerable variance in the organ growth process is tolerable. This is almost certainly not the case in the lens, which in addition to fitting comfortably within the eyeball, must also be of the correct size and shape to focus light sharply onto the retina. Furthermore, the lens does not perform its optical function in isolation. Its growth, which continues throughout life, must therefore be coordinated with that of other tissues in the optical train. Here, we review the lens growth process in detail, from pioneering clinical investigations in the late nineteenth century to insights gleaned more recently in the course of cell and molecular studies. During embryonic development, the lens forms from an invagination of surface ectoderm. Consequently, the progenitor cell population is located at the surface and differentiated cells are confined to the interior. The interactions that regulate cell fate thus occur within the obligate ellipsoidal geometry of the lens. In this context, mathematical models are particularly appropriate tools with which to examine the growth process. In addition to identifying key growth determinants, such models constitute a framework for integrating cell biological and optical data, helping clarify the relationship between gene expression in the lens and image quality at the retinal plane.

Keywords

Lens; growth; stochastic; branching process; Notch; Wnt; FGF; mathematical model

1. Introduction

1.1 Schematic eyes hint at the precision with which living eyes are constructed

The Swedish ophthalmologist and physicist Allvar Gullstrand, in work for which he would later receive the Nobel prize, was among the first to devise an anatomically accurate optical model of the eye, the “exact eye” (Ehinger and Grzybowski, 2011). Featuring four spherical

*Corresponding author: bassnett@wustl.edu, Department of Ophthalmology and Visual Sciences, Washington University School of Medicine, 660 S. Euclid Ave, Campus Box 8096, St. Louis, MO 63117. USA.

refractive surfaces and a lens with a non-uniform refractive index, Gullstrand's exact eye was an important advance in understanding ocular image formation.

Optical models utilize input data such as the radius of curvature and asphericity of the lens surfaces and the shape of the lens internal refractive index gradient. Parameters are sometimes specified to the second or third decimal place, raising a simple but rather fundamental question: what processes control the size and shape of the living, biological lens with such evident precision? This is the issue that we will try to address in this paper. Whatever the nature of the growth control mechanisms, they must indeed be robust. For visual creatures such as ourselves, mismatches in the size or shape of optical components would have catastrophic effects on evolutionary fitness, and are presumably subject to strong negative selection.

1.2. Lens growth influences, and is influenced by, the growth of adjacent structures

The lens does not develop in isolation and its presence reciprocally influences the growth of adjacent structures. The freshwater teleost *Astyanax mexicanus* is a case in point. In the wild, *Astyanax mexicanus* exists in two forms: a surface-dwelling form and a cave-dwelling form (Jeffery, 2009). Surface fish have large, prominent eyes. In contrast, cavefish lack eyes. Surprisingly, early eye development is comparable in the two forms. However, by the end of embryogenesis, ocular growth ceases in cavefish and the eye primordium is quickly overgrown by head epidermis, eventually sinking into the orbit. Growth arrest is due to apoptotic cell death in the lens, which subsequently triggers the degeneration of the cornea, iris, and retina. Importantly, transplantation of a surface fish lens into the eye of a cavefish substantially rescues the growth of the other ocular tissues (Yamamoto and Jeffery, 2000). Thus, in the eye of *Astyanax mexicanus*, the lens is required for the successful development of other structures.

In chicken embryos, surgical removal of the lens causes a marked decrease in the overall growth of the eye (Coulombre and Coulombre, 1964), perhaps secondary to reduced production of vitreous humor, for which the presence of a lens is required (Coulombre and Herrmann, 1965). In mouse embryos, genetic ablation experiments (utilizing lens-expressed diphtheria toxin) demonstrate that lens growth defects generally result in microphthalmia (Breitman et al., 1987). Similarly, conditional deletion of the p110α catalytic subunit of phosphoinositide 3-kinase (PI3K) in the lens causes reduced lens growth and a proportionate decrease in the size of the globe (Sellitto et al., 2016). These results suggest that the lens exerts powerful qualitative and quantitative effects on tissues in the developing eye. Often, in the absence of a lens, other tissues do not develop at all or, if they do, they degenerate subsequently. If, on the other hand, the lens is present but grows too slowly, the overall growth of the eye is hindered, resulting in microphthalmia. Thus, in addition to determining lens size and shape, the lens growth process profoundly influences the development of the rest of the eye.

Clues to the identity of the intrinsic signaling pathways that regulate lens size and shape have recently emerged (see Section 5) but experiments conducted in the 1960's indicate that extra-lenticular factors also have important roles (Figure 1). For example, it is possible to remove a lens from a five-day-old (E5) chicken embryo and replace it with two lenses from

donor embryos of the same age (Coulombre and Coulombre, 1969). The donor lenses can be positioned perpendicular to their original orientation. Remarkably, by E14, in both size and shape, donor lenses grow to resemble a single lens from an un-operated eye. Based on the results of such experiments, it is likely that the form of the embryonic lens is influenced substantially by mechanisms extrinsic to the lens.

2. Macroscopic aspects of lens growth

2.1 Lens size

For most tissues in the body, growth ceases at maturity, which, in humans, occurs early in the third decade of life. In tissues with this so-called determinate growth mode, the high rates of cellular proliferation that characterize early development gradually subside, such that in adults, the rates of cell production and cell death are balanced and cell constancy is achieved. The human eye globe is an example of determinate growth; its maximum external dimensions are attained in the first few years of life (Augusteyn et al., 2012). In contrast, growth of the human lens appears to be indeterminate; its size increasing steadily throughout life (Figure 2 and (Smith, 1883)).

Lenses appear to grow by one of two modes: monophasic or biphasic (Augusteyn, 2007, 2008, 2014a, b). For most species, lens growth is monophasic: rapid during early development but slowing postnatally, approaching an asymptotic maximum by the end of the life span. The composite image of a mouse lens at various stages of development (Figure 3) is a visual representation of the monophasic growth mode.

Monophasic growth is described by a logistic-like function of the form

$$W = Wm\, e^{-\frac{k}{A}} \quad (1)$$

where W is lens weight, Wm is the maximum asymptotic weight, k is the growth constant, and A is time since conception. In an analysis of 14,000 lenses from 130 species, Augusteyn concluded that all but six species exhibited monophasic growth (Augusteyn, 2014a), characterized by diminishing growth rates at later time points (Figure 4A). On logistic plots of lens weight (Figure 4B), the slope of line of best fit gives the growth constant k (see equation (1)) and the y intercept provides the asymptotic maximum. Furthermore, by simply drying lenses, the fraction of solid material can be determined and the rate of increase in dry weight compared with the increase in wet weight. For the example of the rat lens (Figure 4C), it is evident that dry weight accumulates more rapidly than wet weight. Consequently, the proportion of solid material in the lens increases over time (Figure 4D). In lenses from newborn rats, dry material constitutes approximately 20% of the mass, but this value more than doubles by the time the animal is six months old. In the 32 species for which both lens wet weight and dry weight data were available, Augusteyn noted that $k_{(\text{dry weight})}$ generally exceeded $k_{(\text{wet weight})}$ by 10–20% (Augusteyn, 2014a). Thus, in many species, the proportion of dry weight increases significantly with age. This phenomenon is believed to reflect the time-dependent compaction of fiber cells in the lens interior. The precise mechanism of

cellular compaction remains elusive but the net effect is to extract water from the cytosol of the inner fibers, leading to the concentration of residual protein (Bassnett and Costello, 2016). Importantly, the establishment of intra-lenticular protein gradients (Philipson, 1969) underlies the internal refractive index gradient of the lens, serving to both augment the focusing power of the lens and correct for longitudinal spherical aberration (Pierscionek and Regini, 2012).

The near linear increase in volume of the human lens measured by Priestly Smith (Figure 2) is not compatible with a monophasic growth mode. In fact, humans are one of relatively few species in which lens growth is not well described by a straight line on a logistic plot (Augusteyn, 2014a). Examination of curated data collected from 614 human lenses suggests that human lens growth is biphasic (Augusteyn, 2007). In humans, lens growth in utero and in the immediate postnatal period is asymptotic, leading by the second year of life, to the production of a lens with a mean weight of 149 mg. Thereafter, the lens grows linearly (but slowly), at a rate of about 1.38 mg/year. Human lens growth across the entire life span (from conception to extreme old age) is well described by the following equation

$$Wet\ weight\ (mg) = 1.38\ A_b + 149\ e^{-[e^{(1.6-3\ A_c)}]} \quad (2)$$

Where A_b is age since birth and A_c is age since conception (both in years). This equation was used to fit the growth measurements shown in Figure 5.

2.2 Lens shape

In many species, lens shape appears to be scalable. Fish lenses, for example, are spherical at all stages of development. Similarly, the slightly flattened aspect ratio (sagittal thickness/equatorial diameter ≈ 0.8) of the mouse lens remains relatively constant across the life span (Shi et al., 2012). Here, again, the human lens may be an outlier. Early in embryonic development, the human lens is almost spherical (O'Rahilly, 1975) and remains that way until shortly after birth when, as part of the emmetropization process, it becomes increasingly elliptical, eventually losing ≈20 diopters of refractive power (Figure 6A and 6B). The shape change is the result of an increase in the equatorial diameter and, remarkably, a decrease in sagittal thickness (from about ≈ 4mm at birth to ≈3.3 mm at age 10, according to in vivo measurements (Mutti et al., 1998; Zadnik et al., 1995), and with the minimum falling in the late teens, according to in vitro measurements (Schachar, 2005)). Gross changes in the shape of the human lens during childhood and puberty appear to reflect both compaction and remodeling of fiber cells in the lens interior (Augusteyn, 2017).

During adulthood (>20 years of age) the lens increases in sagittal thickness by about 0.02 mm/year, reaching ≈ 5 mm by 90 years of age (Augusteyn, 2010). The equatorial diameter increases at a similar rate, so that the aspect ratio (approximately 0.5 for human lenses measured in vitro) remains fairly constant throughout adulthood (Rosen et al., 2006). The increase in thickness of the aging human lens is particularly noticeable in Scheimpflug images taken of eyes at different ages (see Figure 6C and 6D, for example). Of note, the shape of the human lens is quite challenging to describe mathematically. In a recent study,

lens shape was defined using a 10th order Fourier series (Urs et al., 2010), while a second study evaluated the suitability of interdependent conic, hyperbolic cosine, and polynomial-based models (Smith et al., 2009).

3. Anatomy of the growth process

3.1 Cellular organization of the vertebrate lens

The lens is a smooth ellipsoidal structure enveloped by a thick basement membrane, the lens capsule (Figure 7A and 7B). An epithelium lines the inner surface of the anterior capsule. The epithelial cells have distinct apical and basal-lateral membrane domains. They are also polarized in the plane of the epithelium (see Section 5.3). Because the lens forms from an invagination of the embryonic ectoderm, the apical membranes of the epithelial cells are directed inward, adjoining the anterior tips of the underlying fiber cells. Lens epithelial cells have a dynamic and complex morphology that varies significantly with age and their location on the lens surface (Shi et al., 2015b). In all cases, the apicolateral membranes have smooth polygonal profiles with well-defined vertices (implying that the apical surface is under tension (Fletcher et al., 2014)). By contrast, basal membranes are irregular and feature lamellipodia-like extensions (Figure 7C). The cellular footprint (i.e., the area of the lens surface covered by an individual epithelial cell) also varies significantly with latitude: the cells of the central epithelium have larger footprints than those closer to the equator (Shi et al., 2015b). Indeed, the variation in cell density with latitude is a remarkably consistent feature of the lens epithelium of all species examined to date (Wu et al., 2015).

The equatorial margin of the epithelium is marked by the presence of meridional rows (MR). MR cells are sometimes included in the epithelial cell population (Rafferty and Rafferty, 1981) but they are actually nascent fibers (Bassnett et al., 2011). The meridional rows are the surface manifestation of the radial cell column organization found in the fiber cell mass (Figure 7B, 7E and (Kuszak et al., 1985)).

Mitosis in the peripheral epithelium results in migration/displacement of cells from the epithelial margin. At the lens equator, exposure of epithelial cells to growth factors present in the vitreous humor triggers their terminal differentiation. The differentiated cells (fiber cells) are characterized by a highly elongated and, in mice, undulating form (Figure 7D). Because of the continuous addition of newly formed fibers to the lens surface, the lens radius increases over time. However, the rate of macroscopic growth reflects a balance between fiber cell deposition at the surface and compaction of extant cells in the lens interior (Bassnett and Costello, 2016).

3.2 The growth engine of the lens: mitosis in the epithelium

Lens growth depends on the provision of new cells. It has long been recognized that cell division is confined to the epithelial layer (Mikulicich and Young, 1963; Von Sallmann et al., 1957) and that the rate of mitosis, the distribution of dividing cells across the epithelium, and the cell cycle length, all depend strongly on age (Shi et al., 2015b; Sikic et al., 2017).

In the embryonic mouse lens, the majority (perhaps all) of the epithelial cells are actively cycling, as evidenced by a Ki67 labeling-index that approaches 100% (Upadhya et al.,

2013). Estimates of cell cycle duration in developing lenses are 8.5–9 h and 8 h in chicks and mice, respectively (Sikic et al., 2017; Zwaan and Pearce, 1971), significantly shorter than the 24 hour cycle times reported for adult lenses (Rafferty and Smith, 1976). The EdU-labeling index in the embryonic lens epithelium is ≈50% (Sikic et al., 2017) a value, which in light of the Ki67 data, probably reflects the fraction of the cycle spent in S-phase. Rapidly dividing epithelial cells spend only a brief period in the G_1 phase of the cycle, providing little opportunity for growth between cell divisions. Consequently, the cytoplasmic volume of embryonic lens epithelial cells is small and cells are packed densely within the epithelial layer. A capillary network, the tunica vasculosa lentis, surrounds the developing lens and may help supply the nutrients necessary to support its rapid early growth.

In embryonic lenses, the proliferation rate is relatively uniform across the epithelium (Sikic et al., 2017) but this is not the case in adult lenses, where proliferating cells are most numerous near the periphery. The introduction of confocal microscopy, in conjunction with contemporary S-phase labeling strategies (Salic and Mitchison, 2008), has allowed the distribution of dividing cells to be visualized on the curved surfaces of intact lenses (Bassnett and Shi, 2010; Wiley et al., 2010) and the proliferation index to be calculated as a function of latitude (Shi et al., 2015b). Such analyses have revealed that proliferating cells are distributed throughout a broad swath of the peripheral epithelium (illustrated in Figure 3, quantified in Figure 8). In two-month-old mouse lenses, for example, the region that contains proliferating cells extends ≈750 μm from the lens equator (≈ 45% of the arc length from the equator to the pole). Within this region, most of the cell division occurs in a band of cells located between 100 and 400 μm from the lens equator. Curiously, this region, which is generally referred to as the germinative zone (GZ), includes two clear peaks in labeling index, separated by ≈ 140 μm (Figure 8). At the outermost rim of the epithelium, between the GZ and the MR region, lies a band of cells ≈ 7–10 cell diameters in width, in which the rate of cell division is zero (Mikulicich and Young, 1963; Rafferty and Rafferty, 1981)). This region is called the transition zone (TZ) and is populated by cells actively expressing the cyclin dependent kinase inhibitors $P27^{kip1}$ and $p57^{kip2}$ (Zhang et al., 1998).

3.3 Does the lens epithelium contain adult stem cells?

In the mouse lens, epithelial cell mitosis provides a surfeit of cells, sufficient to populate the expanding epithelial surface while providing enough nascent fiber cells (as many as 15,000 per day, during early development (Sikic et al., 2017)) to support the overall growth of the tissue. Even in lenses of aged mice, where the epithelial cell population is stable (at ≈ 43,000 cells (Bassnett and Shi, 2010)) and where rates of mitosis are diminished in comparison to younger lenses, ongoing proliferation results in the addition of 200–400 cells per day to the fiber cell mass (Rafferty and Rafferty, 1981; Shi et al., 2015b). In many species, it is possible to completely remove the fiber cells from the lens and, provided that the epithelium is spared, proliferation and differentiation of the remaining epithelial cells can reconstitute the entire lens (Gwon, 2006). Recently, the regenerative ability of human lens epithelial cells has been harnessed to regrow lenses in situ, a novel alternative to conventional extracapsular cataract surgery (Lin et al., 2016). These observations reinforce the notion that the lens epithelium retains the lifelong capacity for self-renewal. Since self-renewal is a defining property of stem cells, a number of investigators have asserted that the

lens epithelium contains a contingent of adult stem cells (Lin et al., 2016; Oka et al., 2010; Rafferty and Rafferty, 1981; Yamamoto et al., 2008; Zhou et al., 2006).

Stem cells are generally considered to have the following characteristics: they are usually located in a stem cell niche, they are often relatively undifferentiated cells that divide infrequently, and they have unlimited replicative ability (Seaberg and van der Kooy, 2003). Classically, stem cells are multipotent. In the hematopoietic system, for example, stem cells are located at the apex of a hierarchy that generates erythroid, megakaryocytic, lymphoid and myeloid lineages (Spangrude et al., 1988). In the eye, corneal limbal stem cells fulfill most of the above criteria, although they are unipotent rather than multipotent.

In many settings, stem cells divide infrequently and, as a result, can be identified on the basis of their ability to retain S-phase labels such as ^{3}H-thymidine. The lens epithelium contains such “label retaining cells”. In mice labeled continuously with ^{3}H-thymidine in utero, 13% of lens epithelial cells contain detectable levels of ^{3}H-thymidine when examined four months later and, of these, 1–2% percent are heavily labeled (Zhou et al., 2006). The heavily labeled cells are restricted to the central portion of the epithelium. Lightly labeled cells are found in both the central epithelium and the proliferative regions near the equator. By analogy with other self-renewing systems, Zhou and colleagues have suggested that the heavily labeled cells are lens stem cells, the lightly labeled cells are stem cells/transit amplifying cells, and the unlabeled cells are transit amplifying cells (Zhou et al., 2006). In many self-renewing systems, injury triggers stem cell replication as part of the wound healing response (Lehrer et al., 1998). Similarly, label-retaining cells in the lens epithelium proliferate in response to injury. A small penetrating wound to the central epithelium, for example, stimulates otherwise quiescent cells to reenter the cell cycle (Harding et al., 1979; Zhou et al., 2006) and the same cell population will proliferate in organ culture if exposed to appropriate mitogens (Harding et al., 1968).

Finally, lens epithelial cells express proteins that play important roles in other stem cell-based systems. For example, stem-cell maintenance often depends on the activity of methyltransferases. Methylation is one of the best studied epigenetic modifications and enables cells to retain a cellular memory over repeated cycles of division. In the epidermis, methyltransferase activity is important in maintaining stem cell function and is down regulated during differentiation (Sen et al., 2010). DNMT1, one of three classes of methyltransferases, is essential for the maintenance of stem/progenitor cells in mammary tissue (Pathania et al., 2015). In the mouse lens, conditional knockout of *Dnmt1* results in epithelial cell apoptosis. Those lens cells that escape *Dnmt1* inactivation divide rapidly to repopulate the depleted epithelium, implying that *Dnmt1* is involved in epithelial cell self-renewal (Hoang et al., 2016). Other adult stem cell markers are expressed in the lens epithelium, for example *SOX2* (Arnold et al., 2011) and *Bmi1* (Lin et al., 2016). Unlike somatic cells, stem cells express telomerase activity, which prevents the telomere shortening that would otherwise accompany repeated rounds of cell division (Marion and Blasco, 2010). Notably, lens epithelial cells express TERT (telomerase reverse transcriptase) activity (Colitz et al., 1999).

Although evidence supports the notion that the lens epithelium contains a distinct stem cell population, there are also observations that run counter to that view. First, stem cells, by definition, are capable of extensive replication in vivo or in vitro. It is well established, however, that cultured lens epithelial cells show only limited growth capacity (Andley et al., 1994; Reddan et al., 1982) and that even this modest ability declines with age (Power et al., 1993). Typically, in lens epithelial cultures, cell division ceases after 5–7 population doublings (Jacob, 1987). Second, the lens epithelium lacks an obvious stem cell niche analogous, for example, to the palisades of Vogt of the corneal limbus, which are believed to harbor the corneal stem cell population (Tseng et al., 2016). Third, lineage tracing experiments in the lens have failed to identify putative stem cells. In this regard, it is interesting to compare the behavior of the lens epithelium with that of the nearby corneal epithelium, a system in which a stem cell population has been identified unequivocally. The two systems are similar in several respects. Both the cornea and lens are derived from the ectoderm and, in both cases; progenitor cell division produces a proliferating, migratory cell population that traverses a basement membrane substrate (Bowman's membrane in the case of the cornea and the capsule in the case of the lens) before terminally differentiating. Using tamoxifen induced cre-recombinase activity, individual cells (and their progeny) in the cornea or lens can be tagged permanently with green fluorescent protein (GFP; see (Shi and Bassnett, 2007)) allowing cell fate to be visualized directly. Figure 9 shows the results of such an experiment in the mouse eye. A few days after tamoxifen administration, scattered cells in the cornea and lens begin to express GFP (Figure 9A). The labeling conditions are adjusted such that cre-mediated recombination occurs in a subset (1–5%) of cells only. Cells throughout the cornea are labeled initially, including stromal cells, endothelial cells and epithelial cells. However, the number of GFP-positive cells in the epithelium decreases over time, as cells are desquamated from the ocular surface. Four months after tamoxifen treatment, the corneal epithelium is largely devoid of GFP-positive cells. The exception is the presence of one or more streams of labeled cells emanating from the limbus and extending toward the center of the cornea (Figure 9B, 9C). Such a labeling pattern reflects the presence of a stem cell population at the limbus, as noted by others using similar visualization strategies (Collinson et al., 2002; Di Girolamo et al., 2015). Presumably, the presence of streams of GFP-tagged cells indicates that a tamoxifen-induced recombination event occurred in an individual limbal stem cell. The stream consists of daughter cells produced by the GFP-positive stem cell. Under these labeling conditions, cellular streams, projecting from the limbus (Figure 9B, 9C) are observed in approximately half of all eyes from tamoxifen-treated animals.

Tamoxifen treatment also triggers GFP expression in scattered lens epithelial cells (Figure 9D). Cells that were close to the lens equator at the time of treatment soon differentiate into GFP-positive fiber cells. Cells that were in the proliferative zones at the time of treatment continue their migration toward the equator, dividing (perhaps several times) en route, resulting in the formation of clonally related cell clusters (Figure 9E, 9F). The clusters of epithelial cells eventually reach the equator and differentiate, leading to the formation of broad fluorescent stripes in the fiber mass, as the GFP-labeled fibers are internalized into the body of the lens. Significantly, streams of GFP-labeled cells analogous to those in the cornea are not observed. If label-retaining cells in the central epithelium were the ultimate source of

lens cells, one might expect to see a stream of GFP-positive cells linking such “stem cells” to the internalized fiber cells. To date, no such trails have been observed.

The lineage-tracing data do not support the hypothesis that a distinct stem cell population is maintained in the lens epithelium. The observations are, however, consistent with the view that the entire epithelium represents a single population of progenitor cells, the behavior of which is strongly dependent on cues in the local environment. This arrangement is found in other epithelia. The esophageal epithelium for example, appears to contain a single population of cells. This precursor cell population can either proliferate or differentiate (and be lost from the epithelial surface). Upon wounding, the balance between the two cell fates shifts to favor the production of proliferating cells (Doupe et al., 2012).

If the lens epithelium represents a single progenitor cell population, what regulates the size of this pool of cells? A careful census of the epithelial cell population has revealed that is fluctuates significantly over time (Sikic et al., 2017). In young mouse lenses the population increases rapidly, reaching a maximum value of about 50,000 cells by four weeks of age. Thereafter, the epithelial cell population declines (despite the ongoing increase in lens size) to about 43,000 cells, at which point it stabilizes. Cell death is not a significant factor in the healthy lens epithelium (Rafferty and Rafferty, 1981), so the fluctuating epithelial population presumably reflects the relative rates of cell production in the epithelium and cell loss to the fiber cell compartment. Up until four weeks of age the rate of proliferation exceeds that of differentiation. The situation then reverses temporarily, depleting the epithelial population. From about four months of age onward, the two rates apparently come into equilibrium and the epithelial population stabilizes. The balance between the rate of proliferation and the rate of differentiation may be due in part to the activity of the cyclin-dependent kinase inhibitors $p27^{Kip1}$ and $p57^{Kip2}$, which are active in the peripheral epithelium and appear to have a role in regulating the size of the progenitor cell population. Overactivation of these proteins results in depletion of the lens epithelial population and a concomitant reduction in lens size (Jia et al., 2007). Conversely, inactivation of $p27^{Kip1}$ and $p57^{Kip2}$ promotes the expansion of the progenitor pool and lens overgrowth (Zhang et al., 1998) (see Section 5.2).

3.4 Cancer and the lens

Lens epithelial cells divide throughout life and are also exposed to ultraviolet radiation. Under such conditions it might be expected that lens neoplasms would be quite common but, in humans at least, this is not the case. To the best of our knowledge, there are no reported cases of human lens cancer in the ophthalmological literature (Albert et al., 2015). Transgenic expression of SV40 large T antigen in mouse lens cells leads to cellular transformation and production of both differentiated and undifferentiated lens tumors (Mahon et al., 1987; Nakamura et al., 1989). Thus, it is not that the intraocular environment per se will not support lens tumorigenesis. It has been argued that the large range in lifetime risk for various types of cancer reflects the number of stem cell divisions that occur in a given tissue over the course of a lifetime (Tomasetti and Vogelstein, 2015). According to this theory, somatic mutations underlie cancer development and these accrue largely by chance, during the process of DNA replication. Thus, a quantitative relationship is expected between the integrated number of stem cell divisions in a tissue and lifetime cancer risk for that

tissue. Such a relationship has been tentatively identified (Tomasetti and Vogelstein, 2015). In this regard, it should be noted that the lens has a different growth pattern to other, cancer prone epithelial tissues, such as epidermis or intestinal epithelium. In those systems, differentiated cells are shed constantly from the tissue surface and must be replaced continuously. Moreover, the sheer surface area of the tissues requires an enormous number of cell divisions to maintain. In contrast, the lens is a relatively small structure in which differentiated cells are internalized rather than shed from the surface. Although the lens indeed increases in mass throughout life (Figure 2), its accretive growth mode means that this is achieved through far fewer cell divisions than are required for homeostasis of other epithelial systems.

4 Molecular genetic insights into lens growth regulation

4.1 Human syndromes provide clues to the nature of growth control mechanisms

Clinical conditions in which the size and/or shape of the lens is compromised may provide insights into the mechanisms that regulate normal lens growth. Microspherophakia (a lens that is both too small and too spherical) is a characteristic feature of several inherited conditions in humans, most notably Weill-Marchesani syndrome (WMS). WMS is a rare (1:100,000) genetic disorder characterized by unusually short stature, short fingers (brachydactyly) and distinctive eye abnormalities (including microspherophakia and ectopia lentis). There are three clinically indistinguishable forms of WMS (WMS-1, -2 and -3) and two closely related conditions, Weill-Marchesani-like syndrome (WMLS) and microspherophakia and/or megalocornea with ectopia lentis and with/without secondary glaucoma (MSPKA); in which the eye phenotypes resemble those seen in WMS but other features, for example brachydactyly, are generally absent.

WMS-1 (MIM# 608990) is an autosomal recessive (AR) condition caused by mutations in a disintegrin and metalloproteinase domain-containing protein 10 (*ADAMTS10)*. WMS-2 (MIM# 134797) is an autosomal dominant (AD) condition caused by mutations in Fibrillin 1 (*FBN1*). WMS-3 (MIM# 602091) is an AR condition caused by mutations in latent TGFβ-binding protein 2 (*LTBP2*). WMLS (MIM# 607511) is an AR disorder caused by mutations in *ADAMTS17,* and MSPKA (MIM# 602091) is a recessive condition caused by mutations in *LTBP2*. In almost all cases, the size and shape of the lens is profoundly affected, being somewhat thicker than usual (4.8 mm in WMS patients vs 3.8 mm in age-matched controls (Razeghinejad et al., 2009)) but much smaller in equatorial diameter, such that the border of the lens can usually be visualized through the dilated pupil (Figure 10). Microspherophakic lenses are observed in 94% of patients with AR WMS and 74% with AD WMS (Faivre et al., 2003). Microspherophakia (caused by *LTBP2* mutations) can also occur in isolation (Kumar et al., 2010). There is considerable overlap between the clinical findings in WMS and those in a related condition, geleophysic dysplasia (GPHYSD). GPHYSD-1 (MIM #612277) is an autosomal recessive disease caused by mutations in *ADAMTSL2*, while GPHYSD-2 is a clinically indistinguishable AD condition caused by mutations in *FBN1*. WMS and GPHYSD have traditionally been distinguished on the basis that GPHYSD patients do not present with the ocular symptoms that characterize WMS. However, recent

studies have shown that microspherophakia and lens subluxation are not uncommon in GPHYSD patients (Kochhar et al., 2013; Zhang et al., 2004).

It is noteworthy that many of the genes involved in syndromic microspherophakia are not expressed strongly in the lens itself but, rather, encode proteins found in abundance in the adjoining ciliary zonule. The zonule is the system of radial fibers that extends from the surface of the non-pigmented ciliary epithelium and connects to the lens near its equator. The zonule serves to suspend the lens in the eye (see Figure 7A). Recent proteomic analysis of the human and bovine zonule has shown that Fibrillin 1 and LTBP2 (genes implicated in WMS-2, WMS-3, MSPKA, and GPHYSD-2) are the two most abundant components (de Maria et al., 2017). Neither is strongly expressed in the lens, however (Shi et al., 2013). Similarly, ADAMTSL2 has been detected in the zonule and to a lesser degree in the vitreous humor (de Maria et al., 2017). These clinical observations raise the possibility that the zonule, which constitutes the mechanical linkage between the lens and the wall of the eye, may actively modulate lens growth. In that regard, it may be significant that the attachment point of the zonule directly overlays the germinative region of the lens epithelium (Figure 9 and (Shi et al., 2013)).

Curiously, reports of macrophakia (a lens that is overly large) are extremely rare, although a recent case report of a human patient with congenital glaucoma showed that on extraction the lens was much thicker than usual, with a dry weight that significantly exceeded (73.1 vs. 49.6 mg) that of age-matched controls (Mohamed et al., 2016). One condition in which the lens is invariably larger than usual is diabetes mellitus, as first noted by Huggert (Huggert, 1953) and confirmed subsequently by Brown and Hungerford (Brown and Hungerford, 1982). In Type 1 diabetes, lens thickness increases, and the lens surface radii of curvature are reduced (Adnan et al., 2015b). MRI images suggest that, in addition to an increase in lens thickness, diabetes is associated with a reduction in equatorial diameter so that, in effect, diabetic lenses become more spherical (Adnan et al., 2015a). In a comparative analysis of lens biometry in patients with Type 1 or Type 2 diabetes, lens thickening was observed in Type 1 patients only (Wiemer et al., 2008b). It is unclear if lens enlargement in diabetes reflects a true growth phenomenon (i.e., increased rates of cellular proliferation and/or differentiation) or merely generalized tissue swelling. The degree of thickening of the anterior clear zone (ACZ) of the lens in diabetic lenses is correlated with insulin dose (Sparrow et al., 1990), perhaps indicating a direct influence of the hormone on lens growth (ACZ thickness is thought to reflect the rate of production of new fiber cells). Furthermore, insulin and insulin-like growth factor have been shown to modulate the rate of lens cell proliferation in a number of model systems. In contrast, on the basis of Scheimpflug photographs of diabetic lenses, other investigators have concluded that all regions of the lens, including the nucleus, are expanded (Wiemer et al., 2008a). Because the lens nucleus is usually completed before the onset of diabetes, those authors have proposed that lens expansion is most likely due to tissue swelling, rather than accelerated growth.

Like other basement membranes, the lens capsule is composed of networks of type IV collagen and laminin, interconnected by nidogen (Danysh and Duncan, 2009). In adult tissues, basement membranes are particularly enriched in the collagen IV heterotrimer α3(IV)α4(IV)α5(IV). Mutations in the genes encoding the three collagen subunits

(*COL4A3*, *COL4A4*, and *COL4A5*) can result in Alport syndrome, a condition characterized by kidney disease, hearing loss, and eye abnormalities. In X-linked Alport syndrome, approximately 25% of adult males develop anterior lenticonus, a localized deformation of the lens surface (Colville and Savige, 1997). Lenticonus appears to be secondary to thinning of the anterior capsule (Choi et al., 2005). The notion that the capsule actively molds the lens substance into an appropriate shape is also supported by the results of lens filling experiments (Hettlich et al., 1994; Nishi et al., 1997; Nishi et al., 2014; Parel et al., 1986). Injectable silicone has been put forward as an alternative to the use of conventional intraocular lenses (IOLs) in extracapsular cataract surgery. In this, still experimental technique, the fiber mass is removed and replaced by a liquid polymer, injected through a small hole in the capsule. As the lens fills with polymer, it naturally adopts the correct ellipsoidal shape. Thus, the capsule, a matrix secreted by the epithelium and to a lesser extent the outer layers of fiber cells (Johnson and Beebe, 1984), plays an important role in shaping the lens.

4.2 Lens growth defects in mouse models

Researchers have long used the mouse eye to model ocular development and disease. The lens is affected in numerous mouse mutants but disturbances in size or shape are generally secondary to overt lens pathology. In a few instances, however, a growth retardation phenotype occurs in lenses of otherwise normal appearance, suggesting that the causative mutation has disrupted some aspect of the lens growth regulatory pathway.

Perhaps the best example is the case of mice deficient in the gap junction protein connexin50 (Cx50; encoded by *Gja8*). Cx50 is an abundant component of the lens membrane proteome (Bassnett et al., 2009). As with all gap junction proteins, Cx50 facilitates the intercellular diffusion of small (<1 kDa) molecules between neighboring cells. In the lens, Cx50 is expressed in both the epithelial and fiber cell compartments. Mutations in *Gja8* result in lenses that are too small (Berthoud et al., 2013; Xia et al., 2012). Similarly, targeted disruption of *Gja8* in the lens invariably affects growth, with knockout lenses weighing ≈40% less than wild types (Rong et al., 2002; White et al., 1998). Morphometric analysis of *Gja8*-null lenses indicates that the microphakic phenotype reflects a deficiency in cell number rather than a generalized reduction in cell size (White et al., 1998). Significantly, replacement of Cx50 by another abundant lens connexin, Cx46, does not restore lens growth, suggesting that Cx50 has a specific and indispensable role in growth regulation (White, 2002). In wild type lenses, epithelial cell proliferation surges in the immediate postnatal period. Cx50-mediated cell-cell coupling is maximal during this period, declining thereafter, as it is gradually supplanted by Cx43-mediated coupling (White et al., 2007). In *Gja8*-null lenses the postnatal increase in proliferation does not occur (Sellitto et al., 2004). It is not immediately evident why increased levels of coupling between epithelial cells in the newborn lens should promote cell division, if indeed it does. One possibility is that coupling facilitates the exchange of critical second messengers between cells. Alternatively, the effect of Cx50 on growth could be independent of channel function. It is interesting to note that the C-terminus of Cx50 interacts directly with skp2 (Shi et al., 2015a), an E-3 ubiquitin ligase. Skp2 is part of a complex (SCF^{Skp2}) that controls ubiquitination (and subsequent degradation) of key cell cycle genes, such as $p27^{kip1}$ and $p57^{kip2}$. The interaction of Skp2

with Cx50 at the plasma membrane is thought to mask the nuclear localization signal of Skp2, blocking nuclear translocation and leading to the stabilization of $p27^{kip1}$ and $p57^{kip2}$. The PI3K pathway has been implicated in Cx50 regulation, with increased PI3K signaling leading to specific increases in Cx50-mediated coupling (Martinez et al., 2015). Similarly, lens specific knockout of p110α (the catalytic subunit of PI3K) leads to a reduction in cell-cell coupling, reduced proliferation and a microphakic phenotype similar to that seen in *Gja8*-null lenses (Sellitto et al., 2016).

5 Signaling networks implicated in the regulation of lens size and shape

Lens growth depends on the integrated activity of diffusible autocrine and paracrine signals, juxtacrine interactions, and possibly, mechanotransduction of physical forces exerted by the ciliary zonule or arising from the anisotropic properties of the lens capsule. There is an extensive literature on this topic and interested readers are directed to excellent recent reviews (Lovicu et al., 2011; McAvoy et al., 2016). Here, we will touch briefly on three signaling pathways that appear to directly influence the growth and shape of the lens.

5.1 FGF signaling

The fundamental polarity of the lens (wherein the epithelium is restricted to the anterior surface and fiber cells are located posteriorly) is established early in development, when cells constituting the anterior wall of the lens vesicle differentiate into the lens epithelium and cells of the posterior wall differentiate into fiber cells. Classical lens reversal experiments (Coulombre and Coulombre, 1963, 1969) suggest that tissue polarity is not an autonomous property of the developing lens but rather a consequence of exposure to signals emanating from the posterior segment of the eye. Work from several laboratories, most notably that of McAvoy, demonstrated that the polarizing signal is fibroblast growth factor (FGF). In vitro experiments have shown that exposure to FGF is sufficient to trigger fiber cell differentiation and that the intrinsic fiber promoting activity of vitreous humor is removed on treatment with neutralizing antibodies to FGF (Schulz et al., 1993). More recently, targeted deletion of three of the five known FGF receptors in the developing lens was shown to completely block fiber cell differentiation (Zhao et al., 2008). Although FGF signaling is necessary for fiber differentiation it may not be sufficient, as evidenced by experiments in which inhibitors of bone morphogenetic protein (BMP) signaling are able to block FGF-induced differentiation (Boswell et al., 2008).

The response of explanted lens epithelial cells to FGF exposure is dose-dependent. At high concentrations (40 ng/ml), explanted epithelial cells differentiate into fiber cells, whereas lower concentrations of FGF (0.15 ng/ml) trigger increased rates of cell proliferation, rather than differentiation (McAvoy and Chamberlain, 1989). Significantly, the concentration of FGF in the vitreous humor is substantially higher than in the aqueous humor (Schulz et al., 1993). Together, these observations constitute the basis of the “FGF gradient hypothesis”, which postulates that a posterior/anterior gradient of FGF is the fundamental polarizing signal for lens architecture; inducing fiber cell differentiation below the lens equator and epithelial cell proliferation in the GZ above the equator.

Although a substantial body of evidence supports a central role of FGF signaling in fiber cell differentiation, the role of FGF as an epithelial cell mitogen is less well established. In mice, most of the S-phase cells in the lens epithelium are located in the GZ, a 300 μm-wide swath of the peripheral epithelium (Figure 8). The proliferative behavior of GZ cells is rather complex. Of note, dividing cells are not evenly distributed throughout the zone. Instead, they are concentrated in two bands running parallel to the equator (see Figure 8). It is difficult to envisage how such a bimodal distribution might arise through exposure to a gradient of single diffusible factor (i.e., FGF). Lens epithelial cells express several growth factor receptors, and a number of mitogens including, for example, insulin-like growth factor-1 (Arnold et al., 1993) and platelet derived growth factor D (Ray et al., 2005), have been detected in aqueous humor. Consistent with these observations, explant studies in rats have shown that cultured epithelial cells proliferate rapidly following exposure to aqueous humor or purified growth factors. In either case, proliferation requires activation of the ERK1/2 and PI3K/Akt signaling pathways (Iyengar et al., 2006). No single growth factor receptor inhibitor (including SU5402, an inhibitor of FGF receptors) is able to block completely the endogenous growth promoting activity of aqueous humor (Iyengar et al., 2009), suggesting that the control of cell proliferation in the lens epithelium may involve signaling by several mitogens, operating through multiple receptor tyrosine kinases.

5.2 Notch signaling

Notch signaling is an evolutionarily conserved juxtacrine (cell-to-cell contact) pathway that regulates a wide range of cell-fate decisions, including maintenance of stem and progenitor cell populations (Hori et al., 2013). Notch receptors are single pass transmembrane proteins encoded by four different genes (*Notch1–4*). Notch 2 and 3 are expressed particularly strongly in the lens epithelium (Lindsell et al., 1996; Saravanamuthu et al., 2012). There are four functional Notch ligands (Delta-like ligand 1 (Dll1), Dll4, Jag1, Jag2) in mammals, all of which are also single-pass membrane proteins. In the lens, Jag1 is expressed predominantly in differentiating fiber cells (Dawes et al., 2014; Jia et al., 2007; Jones et al., 2000; Le et al., 2009; Lindsell et al., 1996; Rowan et al., 2008). In the canonical Notch signaling pathway, ligand binding results in metalloprotease-mediated cleavage and shedding of the extracellular domain of the Notch receptor. A subsequent cleavage event, mediated by the γ-secretase complex, separates the transmembrane segment of the receptor from the active fragment, the Notch intracellular domain (NICD). The NICD subsequently translocates to the nucleus, where it alters gene expression in complex with several cofactors, notably the DNA-binding protein CBF1/Suppressor of Hairless/Lag-1 (CSL; also known as RBP-Jκ). Among genes that are commonly upregulated following Notch activation are members of the *HES* (hairy and enhancer of split) family, which includes the transcriptional repressors Hes1 and Hey2, both of which are expressed in the lens epithelium (Jia et al., 2007; Rowan et al., 2008).

Notch activation generally suppresses differentiation, maintaining progenitor or stem cell proliferation. Conversely, blocking Notch signaling often leads to premature progenitor cell differentiation and consequent depletion of the progenitor cell pool (Aujla et al., 2013).

Evidence for a role of Notch signaling in lens growth came first from experiments using conditional *Rbp-Jκ* knockout mice (Jia et al., 2007). The absence of *Rbp-Jκ* is expected to disrupt signaling through all Notch receptors. Lenses from mutant animals were significantly smaller than controls, implying a role for Notch signaling in lens growth regulation. The Notch effector, Herp2 is expressed in the peripheral epithelium of wild type mice. Herp2 expression is abolished in *Rbp-Jκ*–null lenses, indicating that Notch signaling is required for Herp2 expression in the epithelium. Herp2 generally acts as a transcriptional repressor. In lens, one of its targets appears to be the cyclin-dependent kinase inhibitor $p57^{Kip2}$. Interactions between Herp2 and the $p57^{Kip2}$ promoter actively suppress *p57Kip2* expression. In the absence of Notch signaling in the peripheral epithelium, *p57Kip2* is expressed precociously, leading to premature withdrawal from the cell cycle. Thus, Notch signaling helps to define the border between the mitotically active GZ and the post-mitotic TZ (see Section 3.2). In the absence of Notch signaling, the zonal border shifts anteriorly, the epithelial cell population dwindles, and the production of fiber cells (and hence the overall growth of the lens) is diminished. The central role of $p57^{Kip2}$ in regulating the size of the progenitor cell population is underscored by rescue experiments in which the size of *Rbp-Jκ*–null lenses is normalized if $p57^{Kip2}$ is genetically inactivated.

Experiments on *Rbp-Jk* null mice have been complemented by studies in which specific components of the Notch signaling pathway have been targeted. In keeping with the notion that Notch signaling serves to maintain the progenitor cell pool, constitutive activation of the pathway through expression of NICD leads to a sustained increase in the epithelial S-phase labeling index (Rowan et al., 2008). Moreover, targeted deletion of Notch2, results in a small lens phenotype (Saravanamuthu et al., 2012), as does lens-specific deletion of Jag1 (Le et al., 2009; Le et al., 2012).

Experiments in vitro suggest an interaction between FGF and Notch signaling. Treatment of explanted epithelia with concentrations of FGF sufficient to induce fiber differentiation causes the expression of Jag1 and Notch2 (Saravanamuthu et al., 2009). Further, FGF mediated induction of Jag1 is dependent on Notch signaling (Dawes et al., 2014; Saravanamuthu et al., 2009). Based on these observations, it has been proposed that Notch signaling operates in two distinct modes at the lens equator. In the first mode, unidirectional signaling from the nascent fiber cells to the peripheral epithelium represses fiber differentiation and promotes epithelial proliferation, largely through modulation of $p27^{Kip1}$ and $p57^{Kip2}$. Below the lens equator, in the presence of elevated concentrations of FGF, Notch signaling results in upregulation of Jag1, and $p57^{Kip2}$. Thus, as fiber cell differentiation progresses, Notch signaling switches from lateral inhibition to lateral induction.

5.3 Wnt signaling

The Wnt pathway arose with the metazoan lineages. Wnts are symmetry-breaking proteins that specify the primary body axis during early embryonic development. The Wnt pathway, in brief, consists of large family of lipid-modified ligands (Wnts) which engage receptors (Frizzled) and co-receptors (Lrp5/6) on receiving cells, activating downstream components such as dishevelled (DVL), to elicit appropriate cellular responses. Wnts are relatively short

range signals that usually work in autocrine and paracrine settings. Crucially, Wnt signaling is involved in the regulation of both cell-fate and cell-polarity.

The cell-fate pathway (also referred to as the canonical Wnt pathway) is activated when Wnt ligands bind Frizzled and the Lrp5/6 co-receptor. The key mediator of signaling through the cell-fate pathway is the so-called destruction complex (a multimeric protein complex comprising axin, GSK3β, CK1, and APC) which regulates the turnover of β-catenin. The destruction complex contains two kinases (CK1 and GSK3β) which phosphorylate β-catenin, leading to its continual degradation via the ubiquitin/proteasome pathway. In the presence of Wnt ligand, the Frizzled-Lrp5/6 receptor complex recruits the phosphoprotein DVL, leading to disassembly of the destruction complex. Under these circumstances, the concentration of β-catenin increases in the cell. In the nucleus, β-catenin activates members of the TCF/LEF family of transcription factors, triggering transcription of Wnt target genes (for example, cyclin D1 and c-myc). In many settings, canonical Wnt signaling leads to the specification or maintenance of cell fate. Regulation can occur at multiple points along the signaling pathway but there are two main groups of Wnt antagonists, the soluble Frizzled-related Protein (SFRP) class and the Dickkopf (Dkk) class. At the Frizzled receptor, SFRPs can block Wnt binding, while the Dkk class generally inhibits LRP5/6 coreceptor activity.

Lens epithelial cells appear to express the full repertoire of proteins implicated in canonical Wnt signaling, including multiple Wnt ligands, Frizzled receptors, LRP5/6, DVLs, Dkks and SFRPs (Ang et al., 2004; Chen et al., 2004; Stump et al., 2003). Experimental evidence that Wnt signaling plays an important role in lens morphogenesis was provided by the lens phenotype of mice carrying a null mutation in *Lrp6*. Such animals have microphthalmic eyes with small and malformed lenses, characterized by an incomplete epithelial layer, through which fiber cells are extruded (Stump et al., 2003).

Activity of the canonical cell-fate pathway can be visualized using a TCF/Lef-LacZ transgene reporter. In the lens, the pathway appears to be active uniquely in the embryonic (E11.5–E14.5) epithelium (Liu et al., 2006). Consistent with this notion, targeted knockout of β-catenin in the embryonic epithelium (but not the fiber cell compartment) severely disrupts lens morphology (Cain et al., 2008). Absence of β-catenin from the epithelial layer results in depletion of epithelial cells and an anterior shift in $p57^{Kip2}$ expression, effectively phenocopying the Lrp6 mutant. Conversely, constitutive activation of Wnt/β-catenin signaling in the lens epithelium results in expansion of the epithelial compartment, increased rates of cell division, and delayed $p57^{Kip2}$ expression (Martinez et al., 2009). Together, these observations suggest that the Wnt cell fate pathway has a role in maintaining the lens progenitor cell pool early in development.

Although the cell fate Wnt pathway appears to play little role in the regulation of postnatal lens development (Dawes et al., 2013), increasing evidence suggests that non-canonical Wnt signaling, particularly through the planar cell polarity (PCP) pathway, is important. Originally identified in *Drosophila*, PCP signaling has been implicated in many aspects of vertebrate morphogenesis, including localization of cilia, polarization of hair cells in the inner ear, skin development, and directed cell migration (Davey and Moens, 2017; Yang and Mlodzik, 2015). The PCP pathway organizes cells within the plane of the membrane

(orthogonal to any apical-basal polarity that might be present), allowing cells to orient themselves with respect to global directional cues. The asymmetric distribution of core polarity proteins at the cell membrane constitutes a signal that can be translated into a polarized output. PCP mechanisms involve coupling of adjacent cells, allowing spatial patterns to align, potentially over thousands or even millions of cell diameters. Most of the core proteins in the PCP pathway are integral to or closely associated with adhesion junctions in the plasma membrane. In vertebrates, the core proteins include the Wnt receptor Frizzled (FZ), the transmembrane receptor Van Gogh-like (Vangl) and the atypical cadherin, Celsr. Cytoplasmic components include DVL, Prickle (Pk) and Diversin. In PCP, the core components are arranged asymmetrically. Typically, on one edge of the cell are FZ, Celsr, DVL, and Diversin, while, on the opposite side, are VANGL, Celsr, and Pk.

What is the evidence that the PCP pathway plays a role in lens growth? In invertebrate and vertebrate epithelia, the asymmetric position of the centriole/cilium is believed to reflect the activity of the PCP pathway (Carvajal-Gonzalez et al., 2016). A primary cilium projects from the apical membrane of both epithelial and fiber cells in the lens. The cilium is not randomly positioned; in cells of the central epithelium and fiber cells of the outer cortex, it is located predominantly in the quadrant of the apical membrane closest to the anterior pole of the lens (Sugiyama et al., 2010). Thus, the asymmetric positioning of the cilium is prima facie evidence that the PCP pathway is active in the lens. Similarly, analysis of several core PCP proteins at the apical membranes of elongating fiber cells has revealed that they are not uniformly distributed. In particular, Fz6 and Vangl2 colocalize at the apical-lateral membrane border closest to the anterior lens pole. Conversely, Pk1 is found predominantly on the long sides of the cells, while DVL-2 and -3 are more evenly distributed (Sugiyama et al., 2010).

The role of PCP signaling in the lens has been explored by examining the ocular phenotypes of mice carrying mutations in specific PCP components. In mice homozygous for the *looptail (Lp)* mutation, a mutation in *Vangl2* (Kibar et al., 2001), the gross shape of the lens is distorted. Lens thickness is reduced and the anterior surface is more conical than age-matched controls (Sugiyama et al., 2010). Interestingly, recent studies have shown that targeted knockout of *Vangl2* in the corneal epithelium disrupts the stereotypical patterns of centripetal cell migration (Findlay et al., 2016). In the lenses of *Lp* mice, gross changes in shape were accompanied by disorganized packing of fiber cells and malformations of lens sutures. Similar fiber cell packing defects were observed in *Crsh* mice, which carry a homozygous mutation in *Celsr1*. Changes in lens shape are associated with a failure of fiber cells to adopt a characteristic convex curvature. For example, the expression of a Sfrp2 transgene in lens fiber cells results in gross distortions in lens shape, failure of fiber cells to form the proper convex cell curvature, and defective fiber cell orientation (Chen et al., 2008). It is likely that the some of the phenotype reflects a migration defect, because a strikingly similar effect is observed in mice deficient in *Abi2* (Grove et al., 2004), a protein involved in the regulation of actin dynamics and which is concentrated at the apical membrane of elongating fibers.

Directed migration, cellular alignment and elongation of fiber cells reflects active PCP signaling. Because FZ and DVL are key components of the canonical Wnt pathway and

Wnts (particularly Wnt5a and Wnt 11) have been implicated in the establishment of PCP (Gao, 2012), it is attractive to propose that Wnt gradients constitute global orientation signals in the lens. With this in mind, it is interesting to note that in mixed cultures of fiber and epithelial cells, elongating fibers tend to orient toward islands of epithelial cells (Dawes et al., 2014). In such cultures, explanted cells secrete Wnt5A/B into the culture medium. The presence of exogenous Wnt5A (contributed by a co-cultured Wnt-expressing neuronal cell line) results in an increased proportion of directed outgrowth in nascent fibers. Although gradients of Wnts or other soluble factors are doubtless important, the global organizing signal does not have to be strictly chemical in nature. Mechanical forces can serve as the global orientation cue. For example, in the lens, it is possible that radial tension in the lens capsule could serve to orient cells. Similarly, electric fields, arising from the non-uniform distribution of ion tranlocating pumps and channels in the lens cells (Robinson and Patterson, 1982) could constitute a spatial cue. Work with cultured lens epithelial cells has shown cells orient themselves with respect to electric fields in the medium (Zhao et al., 2012). Moreover, the direction of field-induced cellular migration varied with the origin of the lens cells (i.e., whether they were harvested from the central or peripheral epithelium) (Wang et al., 2003).

6. Modeling lens growth mathematically

6.1 The modeling process

We currently have only a rudimentary understanding of how the behaviors of the myriad component cells of the lens are coordinated to generate a macroscopic structure of the proper size and shape to focus light on the retina. To help bridge this knowledge gap, we have begun to model the growth process mathematically. We note that previous authors have successfully employed mathematical models to gain insights into the biomechanical behavior of the lens (Burd, 2009; Burd and Regueiro, 2015) often with a view to better understanding the accommodative process, but here we focus on lens growth.

The steps necessary to model biological systems were outlined succinctly in a recent edition of this journal (Roberts et al., 2016). First, the essential aspects of the system (in our case, the developing lens) must be identified and the inherent complexity reduced to a manageable level, by means of simplifying assumptions. One must then select between potential phenomenological and mechanistic models. A phenomenological model is often a curve fitting exercise (see, for example, equation (2) and Figure 5) that while useful, provides limited insight into the underlying cellular processes. In contrast, in formulating mechanistic models, an attempt is made to model the relevant behavior of the various components, in the expectation that realistic system level behavior will be an emergent property. Nascent models are benchmarked against empirical data sets. Quite often, models fail because of discordance between model predictions and empirical measurements. This implies that the initial assumptions on which the model was built should be revisited. The iterative process of model refinement continues until simulations faithfully capture the behavior of the biological system. Robust models can successfully accommodate new information and be validated experimentally. Useful models help suggest and test new hypotheses.

6.2 A stochastic growth model of the lens

We have used extant data on lens size, shape, and cellular population dynamics to formulate a branching process-based model of mouse lens growth. The model is built on a number of simplifying assumptions, which are enumerated briefly here.

1. We assume that lens growth is stochastic in nature. It is possible to envisage a process by which a structure such as the lens could be built deterministically. However, for that to be the case, the lineage of each lens cell would have to be controlled from the outset. This is plausible in systems with relatively few cells. During the development of *C. elegans*, for example, the lineage of each cell appears to be specified (see wormweb.org). However, *C. elegans* contains about one thousand cells, whereas lenses contain of the order of 10^5 (mouse) to 10^6 (human) cells. Deterministic mechanisms in the lens seem unlikely, and in light of modeling results, unnecessary. Note that the assertion that lens growth is stochastic does not imply anything about the cell biological underpinnings of the process. Stochastic, in a modeling sense, means merely that the behavior of individual cells is unpredictable. If we observe a single epithelial cell over a period of one day, for example, it might die during that period, divide, or remain unchanged; we cannot say in advance.

2. We assume that cells operate independently. Thus, for example, the proliferative behavior of an epithelial cell does not influence the behavior of its neighbors. Further, we assume that if we employ a discrete (rather than continuous) model and select an appropriate time interval Δt, the proliferative history of a cell is irrelevant (i.e., that by $t+\Delta t$, the cell is as competent to divide as any other). The independence assumption is difficult to test experimentally. It is, however, possible to show that the distribution of S-phase cells in the epithelium follows the Poisson distribution as expected for randomly distributed elements (Sikic et al., 2015), an observation consistent with the independence assumption.

3. We assume that lens cell division is symmetric. By symmetric, we mean that daughter cells are identical (to each other and to the parent cell). In this context, the discussion about the nature and existence of lens stem cells is relevant (see Section 3.3). If a discrete stem cell population exists in the lens epithelium and if those cells undergo asymmetric cell division (i.e. a mitotic event that generates one stem cell and one non-stem cell) then the model would have to be adjusted.

4. We assume that the lens epithelium comprises a single progenitor cell population (see Section 3.3). Clearly, the proliferative activity of cells in different locations on the lens surface varies widely (Figure 8) but, for the purposes of modeling, we simplify the proliferative behavior considerably. We assume that in adult lenses, the epithelium is divided into four discrete zones with respect to cell proliferation (Figure 11). According to this scheme, the central zone (CZ) is mitotically quiescent (at least in adult lenses). Most cell division takes place in the germinative zone (GZ) a band of cells approximately 300 μm wide near the edge of the epithelium. Between the GZ and CZ is a region of modest proliferation (approximately 5-fold lower than in the GZ). This 400 μm-wide zone is called

the pre-germinative zone (PGZ). Finally, between the GZ and the fiber cell population is a narrow band of post-mitotic epithelial cells, the transition zone (TZ). We assume that the proliferative behavior of an epithelial cell simply reflects the zone in which it is located. Thus, a cell in the GZ is quite likely to divide, whereas a cell in the CZ is not.

5. We assume that the fractional area covered by each of the four zones remains constant. We do not know the processes within the lens or external to it that define the proliferative regions, but we think it is reasonable to expect that those processes will scale with the lens. The implication is that if, for example, the CZ were to cover half of the anterior surface of young lenses then it would also cover half of the anterior surface of older and larger lenses. This assumption has important effects on the expected movement of cells within the epithelium. As the lens grows, its surface area expands. Under our assumption, the zones will expand in parallel and a certain number of cells will be required to fully populate the various zones, if gaps in the epithelial layer are to be avoided. For a zone such as CZ (which does not contain proliferating cells), constituent cells will either need to increase their footprint areas or additional cells must be recruited from the adjacent, mitotically active PGZ. Thus, cells produced within the epithelial layer are required not only for fiber cell production, they may also need to be reapportioned in the epithelial plane to populate the expanding zones. Modeling helps us visualize the immigration and emigration that takes place across the (virtual) zonal borders to maintain cell constancy.

6.3 Model simulations and predictions

We have modeled mouse lens growth from shortly after its formation until the end of life. Branching processes have been employed previously to model organ growth (Azevedo and Leroi, 2001; Kimmel and Axelrod, 2015). The novelty of our approach lies in the analysis of a four zone model, in which the dynamics are represented via four related branching processes with immigration and emigration. The mathematical derivation of the lens growth model has been described in detail (Sikic et al., 2015, 2017). Here, we provide a brief overview of selected modeling results.

Lens growth in the mouse is monophasic (see equation (1) and Figure 3). Our model suggests that the rate of cell production necessary to support the extremely rapid growth observed in the young lens can be achieved only if the cell cycle is abbreviated. At E12, for example, modeling indicates that the epithelial cell cycle last 8 hours, with a 5 hour S-phase (Sikic et al., 2017). This is considerably shorter than the 24 h cell cycle (12 hour S-phase) reported for the adult lens epithelium (Rafferty and Smith, 1976), but consistent with empirical measurements on embryonic lenses (Zwaan and Pearce, 1971).

The overall dimensions of the embryonic lens are small, but the rate at which new fiber cells are produced is striking, with some 15,000 new fiber cells differentiating per day (Figure 12). Later, fiber cell production falls to a few hundred cell per day, a rate maintained until the end of life. The population of the lens epithelium undergoes significant fluctuations over the first few months of life (Shi et al., 2015b). During embryonic and early postnatal stages,

the population burgeons and, by four weeks of age, briefly exceeds 50,000 cells. In the following weeks, the population declines, despite the continual growth of the lens. By 12 weeks of age, the epithelial population stabilizes at about 43,000 cells, and thereafter remains relatively constant. The stochastic model successfully captures this dynamic behavior (Figure 13). The fluctuations in the epithelial cell population reflect the interplay between zonal proliferation rates (which generally decline over time, see Figure 8) and the rate of change in footprint area of cells located at different latitudes in the epithelium. These two parameters have been likened to the two pedals of an automobile; lens growth may be controlled by gently applying pressure to the accelerator (proliferation) or the brake (expanding area of the cellular footprint) (Sikic et al., 2017).

The growth model assumes a zonal organization in which the boundaries between regions are sharp. This is a simplification (see Figure 8), but such an approach allows us to monitor the expected movement of cells across these virtual borders. As shown in Figure 14, the cellular flow is stochastic in nature. Driven by variable rates of mitosis in the proliferative zones, the numbers of cells crossing the borders daily fluctuates significantly. Generally, the direction of cellular migration is toward the equator, as depicted in a physical representation of lens growth, the Penny Pusher model (Shi et al., 2015b). However, sometimes flow can be in the opposite direction. For example, in the period 4–12 weeks, a small proportion of the cells produced in the PGZ emigrate into the CZ. Cellular footprints are smaller in cells located nearer the equator. As a result, the population of the GZ is relatively large. The GZ contains cells with the highest proliferation rate and, as such, constitutes the main growth engine of the lens, supplying a large number of cells (>1000 cells per day during this period) to the TZ and, ultimately, the fiber cell compartment.

From a knowledge of the age-dependent variation in cross-sectional area of individual fiber cells (Sikic et al., 2017), the daily production of new fibers (Figure 12), and the fiber cell population as a function of age (Figure 15A), the rate of macroscopic lens growth may be calculated. Model simulations are close to measured values at early stages, but there is an increasing discrepancy between simulations and empirical measurements at later time points, with the model predicting an aged lens that is much larger than actually measured (Figure 15B). The most plausible explanation for the discrepancy is that cells in the living lens become compacted over time (Bassnett and Costello, 2016). While there is a convincing body of evidence data to suggest that compaction is a real phenomenon in the lens, there is very little data on the spatial and temporal details. Thus, in the mouse lens, we do not know which cells are compacted, to what degree they are compacted and when the process begins or ends in various regions of the lens. Until such data are available, we simply apply linear correction factors of 0.025% – 0.030% of the radius per day to compensate for the presumed compaction effect.

The proliferative behavior of individual lens epithelial cells is modeled as a stochastic process and stochastic behavior is evident whenever we examine the growth process at the cellular level (see for example the fluctuating numbers of cells crossing zonal borders daily, Figure 14). However, at the cell population level or when considering the rate of increase in the overall size of the lens, stochastic behavior is not detectable. Indeed, a striking feature of the growth model is that with regard to the behavior of most macroscopic parameters,

consecutive model simulations are almost superimposable (see Figure 13). Thus, a stochastic model manages to generate an organ structure with a precision that would rival any conceivable deterministic process. How can we explain this observation? The precision of the growth mechanism appears to derive from two elements. The first is simply the law of large numbers. By E14.5, the rate of cell proliferation in the mouse lens epithelium has fallen below 100% (Sikic et al., 2017) and probabilistic models such as ours are applicable. Even at that early developmental stage, the lens epithelium already contains sufficient cells that stochastic fluctuations are unlikely to strongly affect the growth trajectory. As a result, consecutive model runs are expected to be similar to each other. The second mechanism that contributes to growth precision derives from the zonal organization of the lens epithelium. In particular, it is noteworthy that the mitotically active regions (GZ and PGZ) are flanked by mitotically inactive regions (CZ and TZ). This arrangement allows supernumerary cells, produced through stochastic fluctuations in mitotic rate in the GZ or PGZ, to escape the growth process. This cellular buffer has the effect of minimizing the coefficient of variation (i.e., the standard deviation divided by the mean) in the process, beyond that which would have arisen through either the branching process itself (Azevedo and Leroi, 2001) or the law of large numbers (Sikic et al., 2017).

The use of lineage tracers (Figure 9) has revealed the clonal organization of the lens epithelium, consistent with the predictions of physical models of the lens (Shi et al., 2015b) and the results of deep sequencing experiments (Mesa et al., 2016). Clonally related cell clusters emerge during the transit of cells through the proliferative regions (PGZ and GZ) of the epithelium. Expected clone sizes (i.e., number of cells in a cluster) and transit times can be calculated using the stochastic model (Sikic et al., 2017) and compared with empirical observations. It might be expected that clone size would be largest in the young lens, where the rate of cellular proliferation in the epithelium is highest (Figure 8). However, this does not appear to be the case. At all time points clonal clusters are expected to contain <100 cells and this number does not differ markedly between young and old lenses. The lack of age dependence can be attributed to the fact that although the rate of cell proliferation is highest in young lenses, the speed with which cells traverse the proliferative zones is also faster. As a result, there is less time for cells to undergo the number of cell divisions required to produce a large clone. The most important effect of diminished rates of cellular proliferation in older lenses is not a reduction in clone size but, rather, a slowed passage through the PGZ, GZ and TZ. Consider, for example, an epithelial cell located in the PGZ, near the border with the CZ. Proliferation of cells located anterior to the marked cell results in its steady displacement toward the equator and, ultimately, its incorporation into the fiber cell mass. In a two-week-old mouse lens, the total transit time for a cell in such a location is 7 weeks. A cell located in the same relative location in a 6-month-old lens would take about 13 months to reach the fiber cell compartment (Sikic et al., 2017). The lengthening transit time may have implications for the development of certain types of cataract (Sikic et al., 2017).

7. Summary and future directions

In *On The Origin of Species*, Charles Darwin addressed what he called ”organs of extreme perfection”, chief among them, the vertebrate camera eye. Darwin wanted to emphasize that

even such a complex organ as the eye could arise through the stepwise evolutionary process. While few would debate the validity of that argument, we still have only the most rudimentary understanding of how the lens and other ocular components come to acquire their precise physical forms during the course of development. Because the eye is a living optical instrument, it has attracted the attention of researchers working in several disparate fields. For example, specialists in physiological optics have analyzed the process of image formation itself. For such studies, the cellular nature of the lens is of little consequence. Similarly, cell and developmental biologists have concerned themselves with the behavior of the component cells of the lens, investigating the details of crystallin synthesis, for example, or the intricacies of the cytoskeletal system. Only very recently have investigators begun to consider how cellular behavior, in the aggregate, might be harnessed to yield a structure with the appropriate size, shape, and optical characteristics to serve as the adjustable focusing element of the eye.

Mathematical models provide a conceptual framework for such integrative studies. The population dynamics in the epithelial layer can be modeled as a stochastic branching process where the distribution of the number of offspring produced in each zone within a given time interval arises from the probabilities of a particular cell dying, surviving, or dividing. The mathematical branching process that defines the epithelial cell population dynamics takes place on the anterior surface of an ellipsoidal tissue. Daughter cells produced via that process are ultimately ushered into the interior of the lens, causing its volume and surface area to increase. At all times, therefore, a delicate balance must be maintained between the rate of production of cells in the epithelium and their ultimate apportionment between various epithelial and fiber cell fates. Having established a model of lens cell population dynamics (Sikic et al., 2015, 2017), the challenge is to integrate what has been learned about the stochastic behavior of cells and the geometry in which they reside with the emerging understanding of the signaling pathways that determine their fate. This approach may provide insights into inherited conditions, such as Weill-Marchesani syndrome, in which the lens is the wrong size or shape. Some tentative links can already be drawn. For example, in the TZ, the likelihood of a cell dividing is extremely low. Several lines of evidence suggest that this is a direct consequence of Notch regulated expression of cyclin dependent kinase inhibitors ($p27^{Kip1}$ and $p57^{Kip2}$) in cells near the equatorial rim (Jia et al., 2007; Rowan et al., 2008). By regulating the size of the progenitor pool, Notch signaling also directly affects the fraction of the lens surface covered by each zone.

Similarly, in the period immediately after birth, the likelihood of a cell dividing in the GZ region is high. In many cells, activation of the PI3K/AKT pathway promotes cellular proliferation and suppresses differentiation. In the mouse lens, targeting of the PI3K pathway results in a permanent growth deficit, due to reduced epithelial proliferation, suggesting that the probability of a cell dividing is regulated through the PI3K/AKT pathway and possibly MTOR, its downstream effector (Sellitto et al., 2016). As more is learned about the pathways that control lens cell behavior, we will be able to more confidently assign molecular identities to what are currently purely mathematical concepts.

In its current form, our stochastic model relates the rate of production of cells in various regions of the epithelium to the incorporation of fibers in the lens body and the subsequent

radial growth of the lens. The internal structure of the lens is not addressed (beyond populating the equatorial plane with hexagonal cross sections). However, in principle, the three-dimensional lamellar structure of the lens could be included in more physically realistic models which, if they also incorporated the internal refractive index gradient of the lens, would be suitable for optical modeling. Promisingly, optical models are now being combined with data on lens physiological properties, to predict visual outcomes of metabolic perturbations (Donaldson et al., 2017; Lim et al., 2016). Thus, converging mathematical and physical models offer the exciting prospect of achieving one of the holy grails of lens research, forging a meaningful connection between the biology of living lens cells and the quality of the final image on the retina.

Acknowledgments

Supported by National Institutes of Health Grants R01EY09852 and P30 EY02687 (SB), and an unrestricted grant to the Department of Ophthalmology and Visual Sciences from Research to Prevent Blindness. Additional support was provided by a Marie Curie International Outgoing Fellowship within the 7th European Community Framework Programme, FP7-PEOPLE-2013-IOF-622890-MoLeGro (HS). We thank Dr. Robert Augusteyn for his helpful comments on a draft version of this manuscript.

References

Adnan, Pope JM, Sepehrband F, Suheimat M, Verkicharla PK, Kasthurirangan S, Atchison DA. Lens Shape and Refractive Index Distribution in Type 1 Diabetes. Invest Ophthalmol Vis Sci. 2015a; 56:4759–4766. [PubMed: 26218903]

Adnan X, Suheimat M, Efron N, Edwards K, Pritchard N, Mathur A, Mallen EA, Atchison DA. Biometry of eyes in type 1 diabetes. Biomed Opt Express. 2015b; 6:702–715. [PubMed: 25798297]

Albert DM, Phelps PO, Surapaneni KR, Thuro BA, Potter HA, Ikeda A, Teixeira LB, Dubielzig RR. The Significance of the Discordant Occurrence of Lens Tumors in Humans versus Other Species. Ophthalmology. 2015; 122:1765–1770. [PubMed: 26130328]

Andley UP, Rhim JS, Chylack LT Jr, Fleming TP. Propagation and immortalization of human lens epithelial cells in culture. Invest Ophthalmol Vis Sci. 1994; 35:3094–3102. [PubMed: 8206728]

Ang SJ, Stump RJ, Lovicu FJ, McAvoy JW. Spatial and temporal expression of Wnt and Dickkopf genes during murine lens development. Gene Expr Patterns. 2004; 4:289–295. [PubMed: 15053977]

Arnold DR, Moshayedi P, Schoen TJ, Jones BE, Chader GJ, Waldbillig RJ. Distribution of IGF-I and -II, IGF binding proteins (IGFBPs) and IGFBP mRNA in ocular fluids and tissues: potential sites of synthesis of IGFBPs in aqueous and vitreous. Exp Eye Res. 1993; 56:555–565. [PubMed: 7684697]

Arnold K, Sarkar A, Yram MA, Polo JM, Bronson R, Sengupta S, Seandel M, Geijsen N, Hochedlinger K. Sox2(+) adult stem and progenitor cells are important for tissue regeneration and survival of mice. Cell Stem Cell. 2011; 9:317–329. [PubMed: 21982232]

Augusteyn RC. Growth of the human eye lens. Mol Vis. 2007; 13:252–257. [PubMed: 17356512]

Augusteyn RC. Growth of the lens: in vitro observations. Clin Exp Optom. 2008; 91:226–239. [PubMed: 18331361]

Augusteyn RC. On the growth and internal structure of the human lens. Exp Eye Res. 2010; 90:643–654. [PubMed: 20171212]

Augusteyn RC. Growth of the eye lens: I. Weight accumulation in multiple species. Mol Vis. 2014a; 20:410–426. [PubMed: 24715758]

Augusteyn RC. Growth of the eye lens: II. Allometric studies. Mol Vis. 2014b; 20:427–440. [PubMed: 24715759]

Augusteyn RC. On the contribution of the nucleus and cortex to human lens shape and size. Clin Exp Optom. 2017 In Press.

Augusteyn RC, Nankivil D, Mohamed A, Maceo B, Pierre F, Parel JM. Human ocular biometry. Exp Eye Res. 2012; 102:70–75. [PubMed: 22819768]

Aujla PK, Naratadam GT, Xu L, Raetzman LT. Notch/Rbpjkappa signaling regulates progenitor maintenance and differentiation of hypothalamic arcuate neurons. Development. 2013; 140:3511–3521. [PubMed: 23884446]

Azevedo RB, Leroi AM. A power law for cells. Proc Natl Acad Sci U S A. 2001; 98:5699–5704. [PubMed: 11331756]

Bassnett S, Costello MJ. The cause and consequence of fiber cell compaction in the vertebrate lens. Exp Eye Res. 2016

Bassnett S, Shi Y. A method for determining cell number in the undisturbed epithelium of the mouse lens. Mol Vis. 2010; 16:2294–2300. [PubMed: 21139698]

Bassnett S, Shi Y, Vrensen GF. Biological glass: structural determinants of eye lens transparency. Philos Trans R Soc Lond B Biol Sci. 2011; 366:1250–1264. [PubMed: 21402584]

Bassnett S, Wilmarth PA, David LL. The membrane proteome of the mouse lens fiber cell. Mol Vis. 2009; 15:2448–2463. [PubMed: 19956408]

Berthoud VM, Minogue PJ, Yu H, Schroeder R, Snabb JI, Beyer EC. Connexin50D47A decreases levels of fiber cell connexins and impairs lens fiber cell differentiation. Invest Ophthalmol Vis Sci. 2013; 54:7614–7622. [PubMed: 24204043]

Boswell BA, Overbeek PA, Musil LS. Essential role of BMPs in FGF-induced secondary lens fiber differentiation. Dev Biol. 2008; 324:202–212. [PubMed: 18848538]

Breitman ML, Clapoff S, Rossant J, Tsui LC, Glode LM, Maxwell IH, Bernstein A. Genetic ablation: targeted expression of a toxin gene causes microphthalmia in transgenic mice. Science. 1987; 238:1563–1565. [PubMed: 3685993]

Brown N. The change in lens curvature with age. Exp Eye Res. 1974; 19:175–183. [PubMed: 4442458]

Brown N, Hungerford J. The influence of the size of the lens in ocular disease. Trans Ophthalmol Soc U K. 1982; 102(Pt 3):359–363. [PubMed: 6964281]

Burd HJ. A structural constitutive model for the human lens capsule. Biomech Model Mechanobiol. 2009; 8:217–231. [PubMed: 18622755]

Burd HJ, Regueiro RA. Finite element implementation of a multiscale model of the human lens capsule. Biomech Model Mechanobiol. 2015; 14:1363–1378. [PubMed: 25957261]

Cain S, Martinez G, Kokkinos MI, Turner K, Richardson RJ, Abud HE, Huelsken J, Robinson ML, de Iongh RU. Differential requirement for beta-catenin in epithelial and fiber cells during lens development. Dev Biol. 2008; 321:420–433. [PubMed: 18652817]

Carvajal-Gonzalez JM, Roman AC, Mlodzik M. Positioning of centrioles is a conserved readout of Frizzled planar cell polarity signalling. Nat Commun. 2016; 7:11135. [PubMed: 27021213]

Chen Y, Stump RJ, Lovicu FJ, McAvoy JW. Expression of Frizzleds and secreted frizzled-related proteins (Sfrps) during mammalian lens development. Int J Dev Biol. 2004; 48:867–877. [PubMed: 15558478]

Chen Y, Stump RJ, Lovicu FJ, Shimono A, McAvoy JW. Wnt signaling is required for organization of the lens fiber cell cytoskeleton and development of lens three-dimensional architecture. Dev Biol. 2008; 324:161–176. [PubMed: 18824165]

Choi J, Na K, Bae S, Roh G. Anterior lens capsule abnormalities in Alport syndrome. Korean J Ophthalmol. 2005; 19:84–89. [PubMed: 15929494]

Colitz CM, Davidson MG, Mc GM. Telomerase activity in lens epithelial cells of normal and cataractous lenses. Exp Eye Res. 1999; 69:641–649. [PubMed: 10620393]

Collinson JM, Morris L, Reid AI, Ramaesh T, Keighren MA, Flockhart JH, Hill RE, Tan SS, Ramaesh K, Dhillon B, West JD. Clonal analysis of patterns of growth, stem cell activity, and cell movement during the development and maintenance of the murine corneal epithelium. Dev Dyn. 2002; 224:432–440. [PubMed: 12203735]

Colville DJ, Savige J. Alport syndrome. A review of the ocular manifestations. Ophthalmic Genet. 1997; 18:161–173. [PubMed: 9457747]

Coulombre AJ, Coulombre JL. Lens Development. I. Role of the Lens in Eye Growth. J Exp Zool. 1964; 156:39–47. [PubMed: 14189921]

Coulombre AJ, Herrmann H. Lens development. 3. Relationship between the growth of the lens and the growth of the outer eye coat. Exp Eye Res. 1965; 4:302–311. [PubMed: 5867351]

Coulombre JL, Coulombre AJ. Lens Development: Fiber Elongation and Lens Orientation. Science. 1963; 142:1489–1490. [PubMed: 14077035]

Coulombre JL, Coulombre AJ. Lens development. IV. Size, shape, and orientation. Invest Ophthalmol. 1969; 8:251–257. [PubMed: 5772716]

Danysh BP, Duncan MK. The lens capsule. Exp Eye Res. 2009; 88:151–164. [PubMed: 18773892]

Davey CF, Moens CB. Planar cell polarity in moving cells: think globally, act locally. Development. 2017; 144:187–200. [PubMed: 28096212]

Dawes LJ, Sugiyama Y, Lovicu FJ, Harris CG, Shelley EJ, McAvoy JW. Interactions between lens epithelial and fiber cells reveal an intrinsic self-assembly mechanism. Dev Biol. 2014; 385:291–303. [PubMed: 24211762]

Dawes LJ, Sugiyama Y, Tanedo AS, Lovicu FJ, McAvoy JW. Wnt-frizzled signaling is part of an FGF-induced cascade that promotes lens fiber differentiation. Invest Ophthalmol Vis Sci. 2013; 54:1582–1590. [PubMed: 23385791]

De Maria A, Shi Y, Luo X, Van Der Weyden L, Bassnett S. Cadm1 expression and function in the mouse lens. Invest Ophthalmol Vis Sci. 2011; 52:2293–2299. [PubMed: 21217103]

de Maria A, Wilmarth PA, David LL, Bassnett S. Proteomic analysis of the bovine and human ciliary zonule. Invest Ophthalmol Vis Sci. 2017; 58:573–585. [PubMed: 28125844]

Di Girolamo N, Bobba S, Raviraj V, Delic NC, Slapetova I, Nicovich PR, Halliday GM, Wakefield D, Whan R, Lyons JG. Tracing the fate of limbal epithelial progenitor cells in the murine cornea. Stem Cells. 2015; 33:157–169. [PubMed: 24966117]

Donaldson PJ, Grey AC, Maceo Heilman B, Lim JC, Vaghefi E. The physiological optics of the lens. Prog Retin Eye Res. 2017; 56:e1–e24. [PubMed: 27639549]

Doupe DP, Alcolea MP, Roshan A, Zhang G, Klein AM, Simons BD, Jones PH. A single progenitor population switches behavior to maintain and repair esophageal epithelium. Science. 2012; 337:1091–1093. [PubMed: 22821983]

Ehinger B, Grzybowski A. Allvar Gullstrand (1862–1930)--the gentleman with the lamp. Acta Ophthalmol. 2011; 89:701–708. [PubMed: 22026737]

Faivre L, Dollfus H, Lyonnet S, Alembik Y, Megarbane A, Samples J, Gorlin RJ, Alswaid A, Feingold J, Le Merrer M, Munnich A, Cormier-Daire V. Clinical homogeneity and genetic heterogeneity in Weill-Marchesani syndrome. Am J Med Genet A. 2003; 123A:204–207. [PubMed: 14598350]

Findlay AS, Panzica DA, Walczysko P, Holt AB, Henderson DJ, West JD, Rajnicek AM, Collinson JM. The core planar cell polarity gene, Vangl2, directs adult corneal epithelial cell alignment and migration. R Soc Open Sci. 2016; 3:160658. [PubMed: 27853583]

Fletcher AG, Osterfield M, Baker RE, Shvartsman SY. Vertex models of epithelial morphogenesis. Biophys J. 2014; 106:2291–2304. [PubMed: 24896108]

Gao B. Wnt regulation of planar cell polarity (PCP). Curr Top Dev Biol. 2012; 101:263–295. [PubMed: 23140633]

Grove M, Demyanenko G, Echarri A, Zipfel PA, Quiroz ME, Rodriguiz RM, Playford M, Martensen SA, Robinson MR, Wetsel WC, Maness PF, Pendergast AM. ABI2-deficient mice exhibit defective cell migration, aberrant dendritic spine morphogenesis, and deficits in learning and memory. Mol Cell Biol. 2004; 24:10905–10922. [PubMed: 15572692]

Gwon A. Lens regeneration in mammals: a review. Surv Ophthalmol. 2006; 51:51–62. [PubMed: 16414361]

Harding CV, Harding D, Susan S. Control of Cell-Proliferation in Rabbit Lens Epithelium. Ophthalmic Res. 1979; 11:264–275.

Harding CV, Wilson WL, Wilson JR, Reddan JR, Reddy VN. Triggering of the cell cycle of an organized tissue in vitro. J Cell Physiol. 1968; 72:213–220. [PubMed: 5724571]

Hettlich HJ, Lucke K, Asiyo-Vogel MN, Schulte M, Vogel A. Lens refilling and endocapsular polymerization of an injectable intraocular lens: in vitro and in vivo study of potential risks and benefits. J Cataract Refract Surg. 1994; 20:115–123. [PubMed: 8201558]

Hoang TV, Horowitz ER, Chaffee BR, Qi P, Flake RE, Bruney DG, Rasor BJ, Rosalez SE, Wagner BD, Robinson ML. Lens development requires DNMT1 but takes place normally in the absence of both DNMT3A and DNMT3B activity. Epigenetics. 2016:1–14.

Hori K, Sen A, Artavanis-Tsakonas S. Notch signaling at a glance. J Cell Sci. 2013; 126:2135–2140. [PubMed: 23729744]

Huggert A. The appearance of the band of disjunction of the lens in diabetes mellitus. Acta Ophthalmol (Copenh). 1953; 31:227–234. [PubMed: 13079727]

Iyengar L, Patkunanathan B, Lynch OT, McAvoy JW, Rasko JE, Lovicu FJ. Aqueous humour- and growth factor-induced lens cell proliferation is dependent on MAPK/ERK1/2 and Akt/PI3-K signalling. Exp Eye Res. 2006; 83:667–678. [PubMed: 16684521]

Iyengar L, Patkunanathan B, McAvoy JW, Lovicu FJ. Growth factors involved in aqueous humour-induced lens cell proliferation. Growth Factors. 2009; 27:50–62. [PubMed: 19085197]

Jacob TJ. Human lens epithelial cells in culture: a quantitative evaluation of growth rate and proliferative capacity. Exp Eye Res. 1987; 45:93–104. [PubMed: 3653288]

Jeffery WR. Chapter 8. Evolution and development in the cavefish Astyanax. Curr Top Dev Biol. 2009; 86:191–221. [PubMed: 19361694]

Jia J, Lin M, Zhang L, York JP, Zhang P. The Notch signaling pathway controls the size of the ocular lens by directly suppressing p57Kip2 expression. Mol Cell Biol. 2007; 27:7236–7247. [PubMed: 17709399]

Johnson MC, Beebe DC. Growth, Synthesis and Regional Specialization of the Embryonic Chicken Lens Capsule. Experimental Eye Research. 1984; 38:579–592. [PubMed: 6468538]

Jones EA, Clement-Jones M, Wilson DI. JAGGED1 expression in human embryos: correlation with the Alagille syndrome phenotype. J Med Genet. 2000; 37:658–662. [PubMed: 10978356]

Kibar Z, Vogan KJ, Groulx N, Justice MJ, Underhill DA, Gros P. Ltap, a mammalian homolog of Drosophila Strabismus/Van Gogh, is altered in the mouse neural tube mutant Loop-tail. Nat Genet. 2001; 28:251–255. [PubMed: 11431695]

Kimmel, M., Axelrod, DE. Branching processes in biology. 2. Springer; New York: 2015.

Kochhar A, Kirmani S, Cetta F, Younge B, Hyland JC, Michels V. Similarity of geleophysic dysplasia and Weill-Marchesani syndrome. Am J Med Genet A. 2013; 161A:3130–3132. [PubMed: 24214363]

Kumar A, Duvvari MR, Prabhakaran VC, Shetty JS, Murthy GJ, Blanton SH. A homozygous mutation in LTBP2 causes isolated microspherophakia. Hum Genet. 2010; 128:365–371. [PubMed: 20617341]

Kuszak JR, Macsai MS, Bloom KJ, Rae JL, Weinstein RS. Cell-to-cell fusion of lens fiber cells in situ: correlative light, scanning electron microscopic, and freeze-fracture studies. J Ultrastruct Res. 1985; 93:144–160. [PubMed: 3879764]

Le TT, Conley KW, Brown NL. Jagged 1 is necessary for normal mouse lens formation. Dev Biol. 2009; 328:118–126. [PubMed: 19389370]

Le TT, Conley KW, Mead TJ, Rowan S, Yutzey KE, Brown NL. Requirements for Jag1-Rbpj mediated Notch signaling during early mouse lens development. Dev Dyn. 2012; 241:493–504. [PubMed: 22275127]

Lehrer MS, Sun TT, Lavker RM. Strategies of epithelial repair: modulation of stem cell and transit amplifying cell proliferation. J Cell Sci. 1998; 111(Pt 19):2867–2875. [PubMed: 9730979]

Lim JC, Vaghefi E, Li B, Nye-Wood MG, Donaldson PJ. Characterization of the Effects of Hyperbaric Oxygen on the Biochemical and Optical Properties of the Bovine Lens. Invest Ophthalmol Vis Sci. 2016; 57:1961–1973. [PubMed: 27096754]

Lin H, Ouyang H, Zhu J, Huang S, Liu Z, Chen S, Cao G, Li G, Signer RA, Xu Y, Chung C, Zhang Y, Lin D, Patel S, Wu F, Cai H, Hou J, Wen C, Jafari M, Liu X, Luo L, Zhu J, Qiu A, Hou R, Chen B, Chen J, Granet D, Heichel C, Shang F, Li X, Krawczyk M, Skowronska-Krawczyk D, Wang Y, Shi W, Chen D, Zhong Z, Zhong S, Zhang L, Chen S, Morrison SJ, Maas RL, Zhang K, Liu Y. Lens regeneration using endogenous stem cells with gain of visual function. Nature. 2016; 531:323–328. [PubMed: 26958831]

Lindsell CE, Boulter J, diSibio G, Gossler A, Weinmaster G. Expression patterns of Jagged, Delta1, Notch1, Notch2, and Notch3 genes identify ligand-receptor pairs that may function in neural development. Mol Cell Neurosci. 1996; 8:14–27. [PubMed: 8923452]

Liu H, Thurig S, Mohamed O, Dufort D, Wallace VA. Mapping canonical Wnt signaling in the developing and adult retina. Invest Ophthalmol Vis Sci. 2006; 47:5088–5097. [PubMed: 17065530]

Lovicu FJ, McAvoy JW, de Iongh RU. Understanding the role of growth factors in embryonic development: insights from the lens. Philos Trans R Soc Lond B Biol Sci. 2011; 366:1204–1218. [PubMed: 21402581]

Mahon KA, Chepelinsky AB, Khillan JS, Overbeek PA, Piatigorsky J, Westphal H. Oncogenesis of the lens in transgenic mice. Science. 1987; 235:1622–1628. [PubMed: 3029873]

Marion RM, Blasco MA. Telomeres and telomerase in adult stem cells and pluripotent embryonic stem cells. Adv Exp Med Biol. 2010; 695:118–131. [PubMed: 21222203]

Martinez G, Wijesinghe M, Turner K, Abud HE, Taketo MM, Noda T, Robinson ML, de Iongh RU. Conditional mutations of beta-catenin and APC reveal roles for canonical Wnt signaling in lens differentiation. Invest Ophthalmol Vis Sci. 2009; 50:4794–4806. [PubMed: 19515997]

Martinez JM, Wang HZ, Lin RZ, Brink PR, White TW. Differential regulation of Connexin50 and Connexin46 by PI3K signaling. FEBS Lett. 2015; 589:1340–1345. [PubMed: 25935417]

McAvoy JW, Chamberlain CG. Fibroblast growth factor (FGF) induces different responses in lens epithelial cells depending on its concentration. Development. 1989; 107:221–228. [PubMed: 2632221]

McAvoy JW, Dawes LJ, Sugiyama Y, Lovicu FJ. Intrinsic and extrinsic regulatory mechanisms are required to form and maintain a lens of the correct size and shape. Exp Eye Res. 2016

Mesa R, Tyagi M, Harocopos G, Vollman D, Bassnett S. Somatic Variants in the Human Lens Epithelium: A Preliminary Assessment. Invest Ophthalmol Vis Sci. 2016; 57:4063–4075. [PubMed: 27537255]

Mikulicich AG, Young RW. Cell Proliferation and Displacement in the Lens Epithelium of Young Rats Injected with Tritiated Thymidine. Invest Ophthalmol. 1963; 2:344–354. [PubMed: 14090724]

Mohamed A, Ali MJ, Parel JA, Augusteyn RC, Sangwan VS. In vitro biometry of a human spherophakia. Clin Exp Optom. 2016

Morales J, Al-Sharif L, Khalil DS, Shinwari JM, Bavi P, Al-Mahrouqi RA, Al-Rajhi A, Alkuraya FS, Meyer BF, Al Tassan N. Homozygous mutations in ADAMTS10 and ADAMTS17 cause lenticular myopia, ectopia lentis, glaucoma, spherophakia, and short stature. Am J Hum Genet. 2009; 85:558–568. [PubMed: 19836009]

Mutti DO, Zadnik K, Fusaro RE, Friedman NE, Sholtz RI, Adams AJ. Optical and structural development of the crystalline lens in childhood. Invest Ophthalmol Vis Sci. 1998; 39:120–133. [PubMed: 9430553]

Nakamura T, Mahon KA, Miskin R, Dey A, Kuwabara T, Westphal H. Differentiation and oncogenesis: phenotypically distinct lens tumors in transgenic mice. New Biol. 1989; 1:193–204. [PubMed: 2562221]

Nishi O, Nishi K, Mano C, Ichihara M, Honda T. Controlling the capsular shape in lens refilling. Arch Ophthalmol. 1997; 115:507–510. [PubMed: 9109760]

Nishi O, Nishi Y, Chang S, Nishi K. Accommodation amplitudes after an accommodating intraocular lens refilling procedure: in vivo update. J Cataract Refract Surg. 2014; 40:295–305. [PubMed: 24461501]

O'Rahilly R. The prenatal development of the human eye. Exp Eye Res. 1975; 21:93–112. [PubMed: 1100417]

Oka M, Toyoda C, Kaneko Y, Nakazawa Y, Aizu-Yokota E, Takehana M. Characterization and localization of side population cells in the lens. Mol Vis. 2010; 16:945–953. [PubMed: 20577594]

Parel JM, Gelender H, Trefers WF, Norton EW. Phaco-Ersatz: cataract surgery designed to preserve accommodation. Graefes Arch Clin Exp Ophthalmol. 1986; 224:165–173. [PubMed: 3949191]

Pathania R, Ramachandran S, Elangovan S, Padia R, Yang P, Cinghu S, Veeranan-Karmegam R, Arjunan P, Gnana-Prakasam JP, Sadanand F, Pei L, Chang CS, Choi JH, Shi H, Manicassamy S, Prasad PD, Sharma S, Ganapathy V, Jothi R, Thangaraju M. DNMT1 is essential for mammary

and cancer stem cell maintenance and tumorigenesis. Nat Commun. 2015; 6:6910. [PubMed: 25908435]

Philipson B. Distribution of protein within the normal rat lens. Invest Ophthalmol. 1969; 8:258–270. [PubMed: 5772717]

Pierscionek BK, Regini JW. The gradient index lens of the eye: an opto-biological synchrony. Prog Retin Eye Res. 2012; 31:332–349. [PubMed: 22465790]

Power W, Neylan D, Collum L. Growth characteristics of human lens epithelial cells in culture. Effect of media and donor age. Doc Ophthalmol. 1993; 84:365–372. [PubMed: 8156856]

Rafferty NS, Rafferty KA Jr. Cell population kinetics of the mouse lens epithelium. J Cell Physiol. 1981; 107:309–315. [PubMed: 7251687]

Rafferty NS, Smith R. Analysis of cell populations of normal and injured mouse lens epithelium. I. Cell cycle. Anatomical Record. 1976; 186:105–114.

Ray S, Gao C, Wyatt K, Fariss RN, Bundek A, Zelenka P, Wistow G. Platelet-derived growth factor D, tissue-specific expression in the eye, and a key role in control of lens epithelial cell proliferation. J Biol Chem. 2005; 280:8494–8502. [PubMed: 15611105]

Razeghinejad MR, Hosseini H, Namazi N. Biometric and corneal topographic characteristics in patients with Weill-Marchesani syndrome. J Cataract Refract Surg. 2009; 35:1026–1032. [PubMed: 19465288]

Reddan JR, McGee SJ, Goldenberg EM, Dziedzic DC. Both human and newborn rabbit lens epithelial cells exhibit similar limited growth properties in tissue culture. Curr Eye Res. 1982; 2:399–405. [PubMed: 6762949]

Roberts PA, Gaffney EA, Luthert PJ, Foss AJ, Byrne HM. Mathematical and computational models of the retina in health, development and disease. Prog Retin Eye Res. 2016; 53:48–69. [PubMed: 27063291]

Robinson KR, Patterson JW. Localization of steady currents in the lens. Curr Eye Res. 1982; 2:843–847. [PubMed: 7187641]

Rong P, Wang X, Niesman I, Wu Y, Benedetti LE, Dunia I, Levy E, Gong X. Disruption of Gja8 (alpha8 connexin) in mice leads to microphthalmia associated with retardation of lens growth and lens fiber maturation. Development. 2002; 129:167–174. [PubMed: 11782410]

Rosen AM, Denham DB, Fernandez V, Borja D, Ho A, Manns F, Parel JM, Augusteyn RC. In vitro dimensions and curvatures of human lenses. Vision Res. 2006; 46:1002–1009. [PubMed: 16321421]

Rowan S, Conley KW, Le TT, Donner AL, Maas RL, Brown NL. Notch signaling regulates growth and differentiation in the mammalian lens. Dev Biol. 2008; 321:111–122. [PubMed: 18588871]

Salic A, Mitchison TJ. A chemical method for fast and sensitive detection of DNA synthesis in vivo. Proc Natl Acad Sci U S A. 2008; 105:2415–2420. [PubMed: 18272492]

Saravanamuthu SS, Gao CY, Zelenka PS. Notch signaling is required for lateral induction of Jagged1 during FGF-induced lens fiber differentiation. Dev Biol. 2009; 332:166–176. [PubMed: 19481073]

Saravanamuthu SS, Le TT, Gao CY, Cojocaru RI, Pandiyan P, Liu C, Zhang J, Zelenka PS, Brown NL. Conditional ablation of the Notch2 receptor in the ocular lens. Dev Biol. 2012; 362:219–229. [PubMed: 22173065]

Schachar RA. Growth patterns of fresh human crystalline lenses measured by in vitro photographic biometry. J Anat. 2005; 206:575–580. [PubMed: 15960767]

Schulz MW, Chamberlain CG, de Iongh RU, McAvoy JW. Acidic and basic FGF in ocular media and lens: implications for lens polarity and growth patterns. Development. 1993; 118:117–126. [PubMed: 7690700]

Seaberg RM, van der Kooy D. Stem and progenitor cells: the premature desertion of rigorous definitions. Trends Neurosci. 2003; 26:125–131. [PubMed: 12591214]

Sellitto C, Li L, Vaghefi E, Donaldson PJ, Lin RZ, White TW. The Phosphoinosotide 3-Kinase Catalytic Subunit p110alpha is Required for Normal Lens Growth. Invest Ophthalmol Vis Sci. 2016; 57:3145–3151. [PubMed: 27304846]

Sellitto C, Li L, White TW. Connexin50 is essential for normal postnatal lens cell proliferation. Invest Ophthalmol Vis Sci. 2004; 45:3196–3202. [PubMed: 15326140]

Sen GL, Reuter JA, Webster DE, Zhu L, Khavari PA. DNMT1 maintains progenitor function in self-renewing somatic tissue. Nature. 2010; 463:563–567. [PubMed: 20081831]

Shi Q, Gu S, Yu XS, White TW, Banks EA, Jiang JX. Connexin Controls Cell-Cycle Exit and Cell Differentiation by Directly Promoting Cytosolic Localization and Degradation of E3 Ligase Skp2. Dev Cell. 2015a; 35:483–496. [PubMed: 26585299]

Shi Y, Barton K, De Maria A, Petrash JM, Shiels A, Bassnett S. The stratified syncytium of the vertebrate lens. J Cell Sci. 2009; 122:1607–1615. [PubMed: 19401333]

Shi Y, Bassnett S. Inducible gene expression in the lens using tamoxifen and a GFP reporter. Exp Eye Res. 2007; 85:732–737. [PubMed: 17905229]

Shi Y, De Maria A, Bennett T, Shiels A, Bassnett S. A role for epha2 in cell migration and refractive organization of the ocular lens. Invest Ophthalmol Vis Sci. 2012; 53:551–559. [PubMed: 22167091]

Shi Y, Tu Y, De Maria A, Mecham RP, Bassnett S. Development, composition, and structural arrangements of the ciliary zonule of the mouse. Invest Ophthalmol Vis Sci. 2013; 54:2504–2515. [PubMed: 23493297]

Shi YR, De Maria A, Lubura S, Sikic H, Bassnett S. The Penny Pusher: A Cellular Model of Lens Growth. Invest Ophth Vis Sci. 2015b; 56:799–809.

Sikic H, Shi Y, Lubura S, Bassnett S. A stochastic model of eye lens growth. J Theor Biol. 2015; 376:15–31. [PubMed: 25816743]

Sikic H, Shi Y, Lubura S, Bassnett S. A full lifespan model of vertebrate lens growth. Royal Society Open Science. 2017

Smith G, Atchison DA, Iskander DR, Jones CE, Pope JM. Mathematical models for describing the shape of the in vitro unstretched human crystalline lens. Vision Res. 2009; 49:2442–2452. [PubMed: 19647765]

Smith P. On the growth of the crystalline lens. Trans Ophthalmol Soc UK. 1883; 3:79–99.

Spangrude GJ, Heimfeld S, Weissman IL. Purification and characterization of mouse hematopoietic stem cells. Science. 1988; 241:58–62. [PubMed: 2898810]

Sparrow JM, Bron AJ, Brown NA, Neil HA. Biometry of the crystalline lens in early-onset diabetes. Br J Ophthalmol. 1990; 74:654–660. [PubMed: 2223701]

Stump RJ, Ang S, Chen Y, von Bahr T, Lovicu FJ, Pinson K, de Iongh RU, Yamaguchi TP, Sassoon DA, McAvoy JW. A role for Wnt/beta-catenin signaling in lens epithelial differentiation. Dev Biol. 2003; 259:48–61. [PubMed: 12812787]

Sugiyama Y, Stump RJ, Nguyen A, Wen L, Chen Y, Wang Y, Murdoch JN, Lovicu FJ, McAvoy JW. Secreted frizzled-related protein disrupts PCP in eye lens fiber cells that have polarised primary cilia. Dev Biol. 2010; 338:193–201. [PubMed: 19968984]

Tomasetti C, Vogelstein B. Cancer etiology. Variation in cancer risk among tissues can be explained by the number of stem cell divisions. Science. 2015; 347:78–81. [PubMed: 25554788]

Tripathi RC, Tripathi BJ. Lens morphology, aging, and cataract. J Gerontol. 1983; 38:258–270. [PubMed: 6841920]

Tseng SC, He H, Zhang S, Chen SY. Niche Regulation of Limbal Epithelial Stem Cells: Relationship between Inflammation and Regeneration. Ocul Surf. 2016; 14:100–112. [PubMed: 26769483]

Upadhya D, Ogata M, Reneker LW. MAPK1 is required for establishing the pattern of cell proliferation and for cell survival during lens development. Development. 2013; 140:1573–1582. [PubMed: 23482492]

Urs R, Ho A, Manns F, Parel JM. Age-dependent Fourier model of the shape of the isolated ex vivo human crystalline lens. Vision Res. 2010; 50:1041–1047. [PubMed: 20338192]

Von Sallmann L, Caravaggio L, Munoz CM, Drungis A. Species differences in the radiosensitivity of the lens. Am J Ophthalmol. 1957; 43:693–704. [PubMed: 13411152]

Wang E, Zhao M, Forrester JV, McCaig CD. Bi-directional migration of lens epithelial cells in a physiological electrical field. Exp Eye Res. 2003; 76:29–37. [PubMed: 12589773]

White TW. Unique and redundant connexin contributions to lens development. Science. 2002; 295:319–320. [PubMed: 11786642]

White TW, Gao Y, Li L, Sellitto C, Srinivas M. Optimal lens epithelial cell proliferation is dependent on the connexin isoform providing gap junctional coupling. Invest Ophthalmol Vis Sci. 2007; 48:5630–5637. [PubMed: 18055813]

White TW, Goodenough DA, Paul DL. Targeted ablation of connexin50 in mice results in microphthalmia and zonular pulverulent cataracts. J Cell Biol. 1998; 143:815–825. [PubMed: 9813099]

Wiemer NG, Dubbelman M, Hermans EA, Ringens PJ, Polak BC. Changes in the internal structure of the human crystalline lens with diabetes mellitus type 1 and type 2. Ophthalmology. 2008a; 115:2017–2023. [PubMed: 18718668]

Wiemer NG, Dubbelman M, Kostense PJ, Ringens PJ, Polak BC. The influence of diabetes mellitus type 1 and 2 on the thickness, shape, and equivalent refractive index of the human crystalline lens. Ophthalmology. 2008b; 115:1679–1686. [PubMed: 18486214]

Wiley LA, Shui YB, Beebe DC. Visualizing lens epithelial cell proliferation in whole lenses. Mol Vis. 2010; 16:1253–1259. [PubMed: 20664699]

Wu JJ, Wu W, Tholozan FM, Saunter CD, Girkin JM, Quinlan RA. A dimensionless ordered pull-through model of the mammalian lens epithelium evidences scaling across species and explains the age-dependent changes in cell density in the human lens. J R Soc Interface. 2015; 12:20150391. [PubMed: 26236824]

Xia CH, Chang B, Derosa AM, Cheng C, White TW, Gong X. Cataracts and microphthalmia caused by a Gja8 mutation in extracellular loop 2. PLoS One. 2012; 7:e52894. [PubMed: 23300808]

Yamamoto N, Majima K, Marunouchi T. A study of the proliferating activity in lens epithelium and the identification of tissue-type stem cells. Med Mol Morphol. 2008; 41:83–91. [PubMed: 18592162]

Yamamoto Y, Jeffery WR. Central role for the lens in cave fish eye degeneration. Science. 2000; 289:631–633. [PubMed: 10915628]

Yang Y, Mlodzik M. Wnt-Frizzled/planar cell polarity signaling: cellular orientation by facing the wind (Wnt). Annu Rev Cell Dev Biol. 2015; 31:623–646. [PubMed: 26566118]

Zadnik K, Mutti DO, Fusaro RE, Adams AJ. Longitudinal evidence of crystalline lens thinning in children. Invest Ophthalmol Vis Sci. 1995; 36:1581–1587. [PubMed: 7601639]

Zhang P, Wong C, DePinho RA, Harper JW, Elledge SJ. Cooperation between the Cdk inhibitors p27(KIP1) and p57(KIP2) in the control of tissue growth and development. Genes Dev. 1998; 12:3162–3167. [PubMed: 9784491]

Zhang X, Boles RG, Law SK, Lin M. Ocular findings in geleophysic dysplasia. J AAPOS. 2004; 8:198–200. [PubMed: 15088061]

Zhao H, Yang T, Madakashira BP, Thiels CA, Bechtle CA, Garcia CM, Zhang H, Yu K, Ornitz DM, Beebe DC, Robinson ML. Fibroblast growth factor receptor signaling is essential for lens fiber cell differentiation. Dev Biol. 2008; 318:276–288. [PubMed: 18455718]

Zhao M, Chalmers L, Cao L, Vieira AC, Mannis M, Reid B. Electrical signaling in control of ocular cell behaviors. Prog Retin Eye Res. 2012; 31:65–88. [PubMed: 22020127]

Zhou M, Leiberman J, Xu J, Lavker RM. A hierarchy of proliferative cells exists in mouse lens epithelium: implications for lens maintenance. Invest Ophthalmol Vis Sci. 2006; 47:2997–3003. [PubMed: 16799045]

Zwaan J, Pearce TL. Cell population kinetics in the chicken lens primordium during and shortly after its contact wth the optic cup. Dev Biol. 1971; 25:96–118. [PubMed: 5557971]

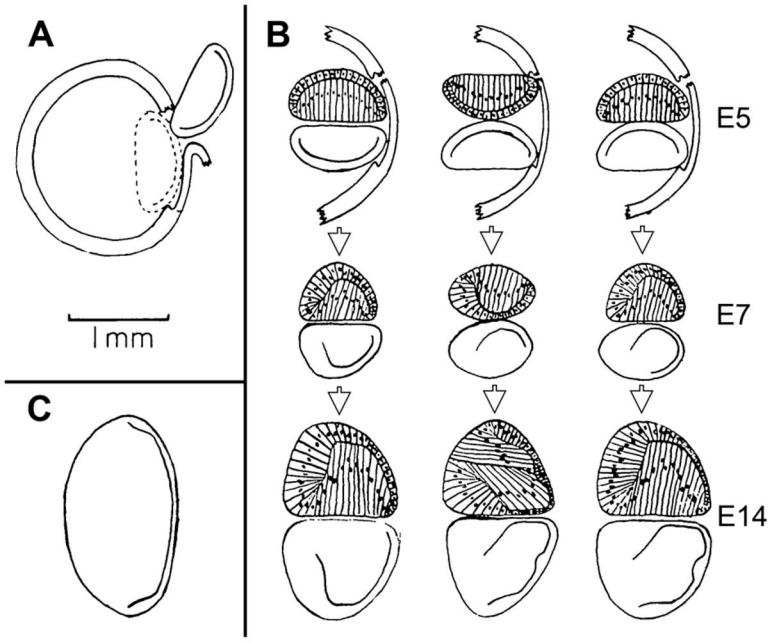

Figure 1.

Extralenticular factors regulate lens size and shape. **A**. The lens is removed from the eye of a 5-day-old (E5) chicken embryo through a limbal incision and replaced with two lenses from donors of the same age. **B**. The donor lenses are oriented orthogonal to the original lens and positioned back-to-back, front-to-front, or front-to-back. Embryos are allowed to develop further and eyes are observed at E7 or E14. Whatever the initial configuration of the donor lenses, by E14 the size and shape of the lens pair closely resemble that of an unoperated lens (C). Diagram adapted from (Coulombre and Coulombre, 1969).

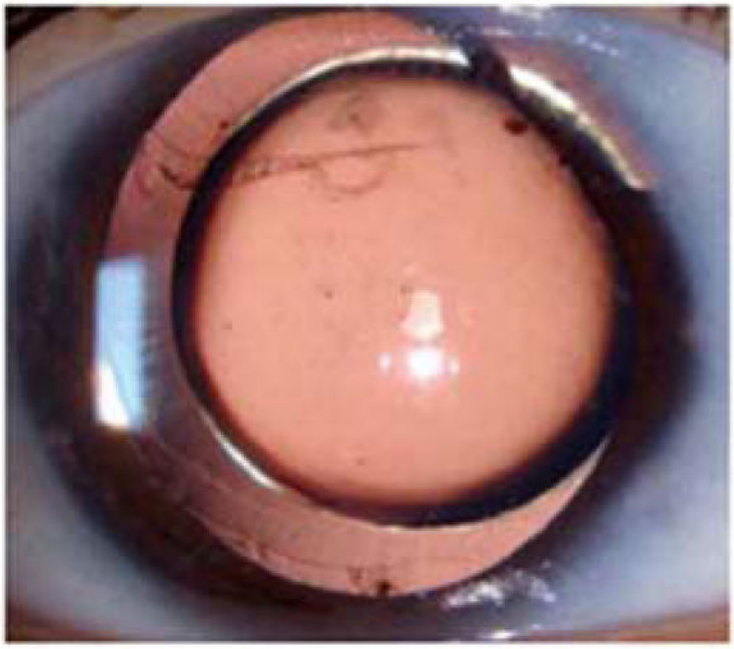

Figure 2.
The volume of the human lens increases throughout life. Reproduced from (Smith, 1883)

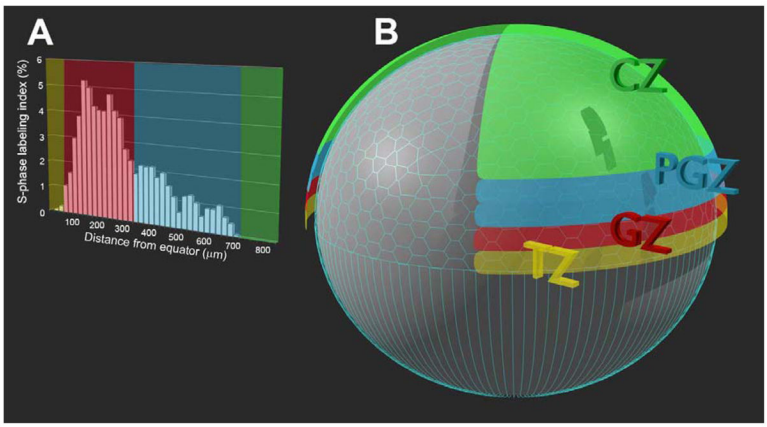

Figure 3.

Monophasic growth in the mouse lens. A “growth wheel” image showing the relative size of the mouse lens at various points in development. Images are two dimensional maximum intensity projections of confocal image stacks viewed from the anterior aspect. The white circle in the center of the image denotes the size of the lens at the time of its formation on embryonic day 10.5 (E10.5). Note the rapid early growth of the lens. Later in the life span, growth is almost imperceptible, despite continual proliferation of cells near the epithelial margin (S-phase nuclei are shown in green; nuclear DNA (red) is labeled with Draq5). Image from (De Maria et al., 2011; Shi et al., 2015b).

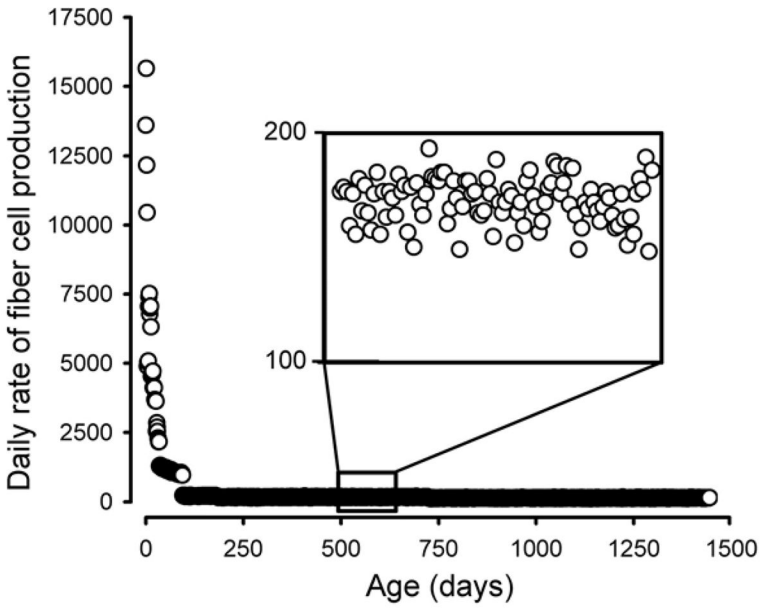

Figure 4.

Monophasic lens growth and tissue compaction. **A**. The wet weight of the rabbit lens increases rapidly over the first six months of life and then tends gradually towards a maximum at later time points. **B**. A plot of log wet weight against 1/age is well fitted by straight line. The magnitude of the slope is equivalent to the growth constant k (see equation (1)) and the y-intercept is the log of the maximum value. **C**. In rats, the slopes of the dry and wet weight data are not parallel, dry weight accumulates more quickly than wet weight. **D**. Dry weight/wet weight ratios increase markedly over the first six months of life (from 18% to 44%), consistent with the notion that water is removed from the cytosol of lens fibers during the process of cellular compaction. Data are adapted from (Augusteyn, 2014a; De Maria et al., 2011)

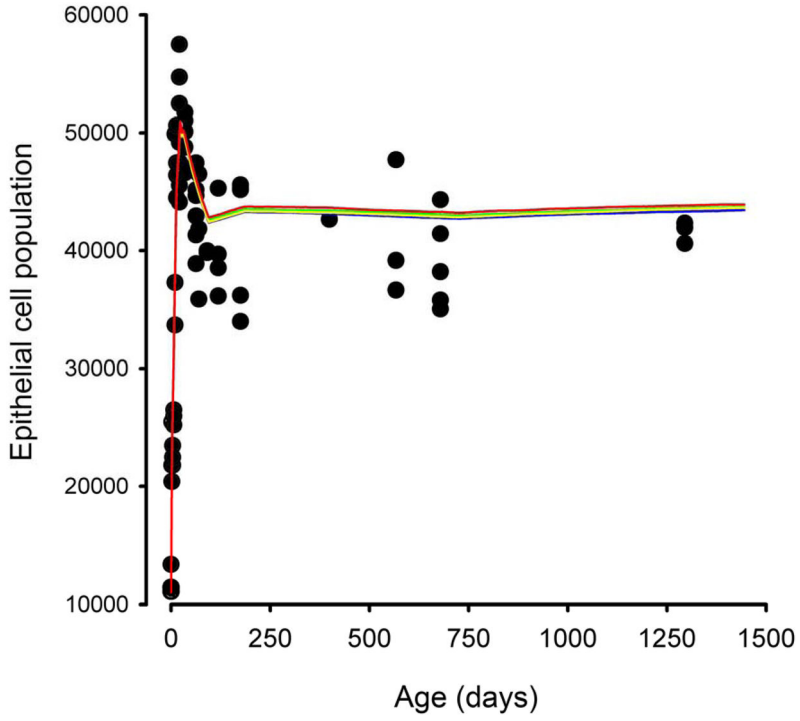

Figure 5.

Biphasic growth of the human lens. Line represents the best fit of equation (2). Data reproduced from (Augusteyn, 2007).

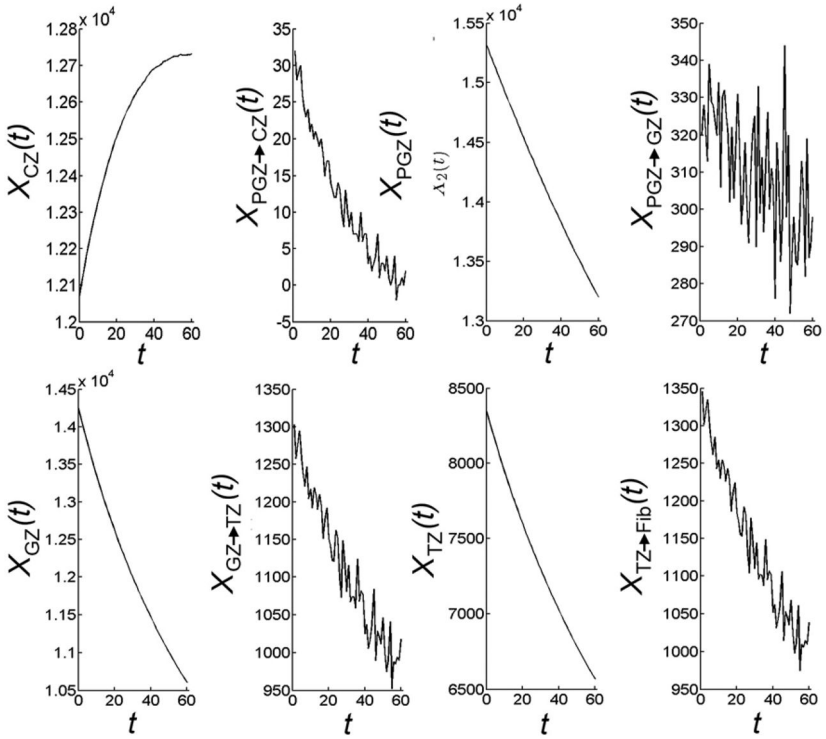

Figure 6.

Age-dependent changes in lens shape and size. Mid-sagittal ocular section from a 3-month-old child (**A**) and an adult (**B**). Note the marked increase in aspect ratio in the older lens. Image adapted from (Tripathi and Tripathi, 1983). Scheimpflug images of the lens of a child (**C**) and an elderly man (**D**). Note the increase in lens thickness in the older eye. Adapted from (Brown, 1974).

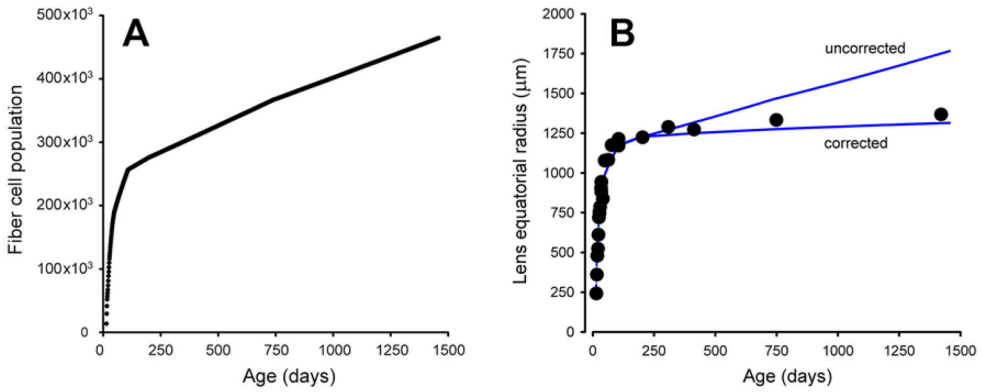

Figure 7.

Cellular arrangement of the mouse lens. **A**. The mouse lens is located centrally within the eye and consists of a bounding capsule (blue), an anterior epithelium (yellow), and a mass of terminally differentiated fiber cells (green). **B**. Cell division (small arrow) in the peripheral epithelium results in the displacement of daughter cells toward the lens equator (large arrow). At the equator, epithelial cells differentiate into fiber cells and are incorporated into the fiber cell mass. Fiber cells have an elongated form and a flattened hexagonal cross section in the equatorial plane (highlighted in white). **C**. A GFP-labeled epithelial cell visualized from the basal aspect within the epithelium of an intact lens. Note the presence of lamellipodia-like processes (*). **D**. Fiber cells in the lens cortex have an undulating morphology with many finger-like protrusions extending from the vertices along the lateral membranes. **E**. In cross section, the fiber cells are arranged in cell columns (four such columns are shown; see also highlighted cells in **B**). Scale bar **C,D,** and **E** = 4μm. Adapted from (Sikic et al., 2015) and (De Maria et al., 2011).

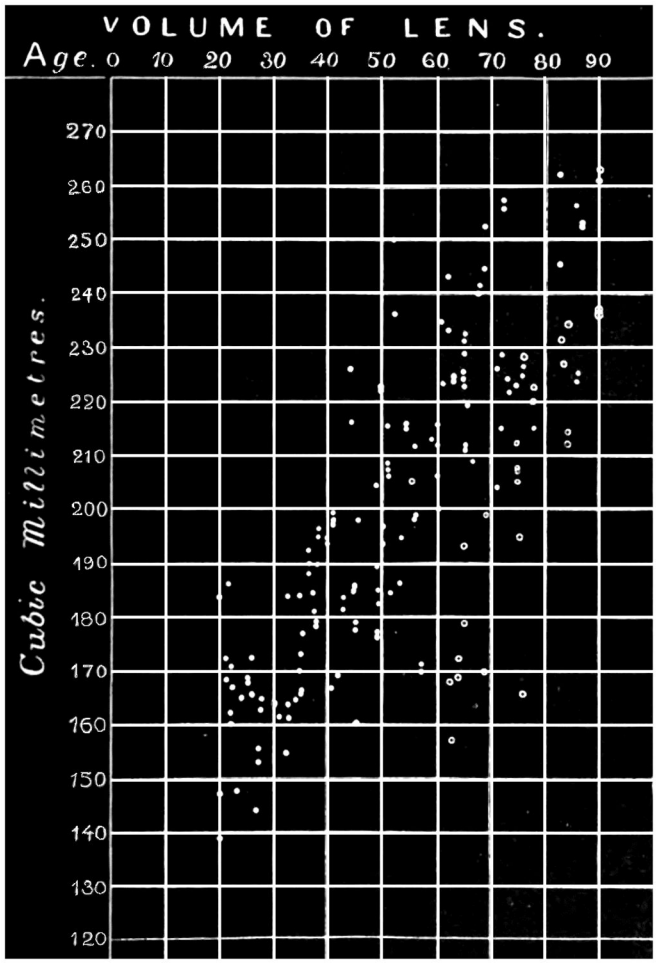

Figure 8.

Variation of S-phase labeling index with distance from the lens equator in 2-weeks-old (orange), 2-months-old (purple), or 2-years-old (brown) mice. Note that at each age two peaks (*) in labeling intensity are evident. Adapted from (Shi et al., 2015b).

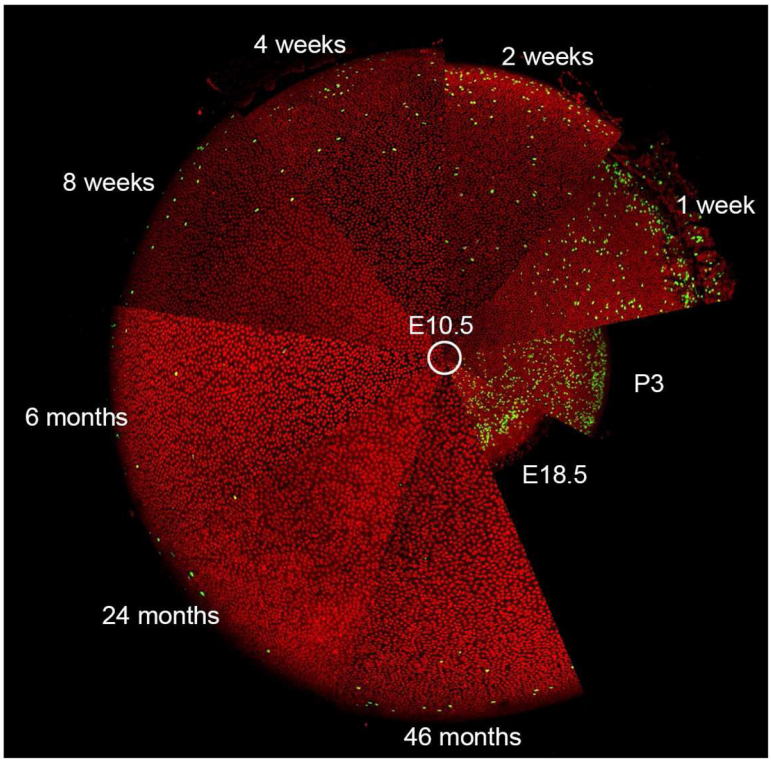

Figure 9.

Lineage tracing identifies stem cells in cornea but not lens. **A**. Tamoxifen treatment results in scattered expression of GFP in cells throughout the ocular surface. **B**. Four months later, almost all GFP-positive cells in the corneal epithelial layer have been lost through desquamation, revealing underlying GFP-positive endothelial cells and keratocytes. The only labeled cells in the epithelial layer are located in a stream (arrowed in **B**) emanating from the limbus (L) and extending toward the center of the cornea. **C**. At higher magnification, individual GFP-positive basal cells are visible. In lenses, tamoxifen induced recombination occurs in epithelial cells only. **D**. One week after tamoxifen treatment, individual GFP-positive epithelial cells (Epi) are visible above the lens equator (Eq). During the intervening period, some GFP-positive epithelial cells have differentiated into fiber cells (Fib). **E**. Four months after tamoxifen treatment, individual GFP-positive epithelial cells are rarely observed near the lens equator (although some are present at the anterior pole (AP) of the lens). In the peripheral epithelium, positively labeled cells are present in clusters of twenty to fifty cells. One such cluster is boxed in **E** and shown at higher magnification in **F**. The broad fluorescent stripes visible in the lens (E) are groups of fluorescent fiber cells formed by the simultaneous differentiation of GFP-labeled epithelial cell clusters. In the lens epithelium, streams of cells resembling those detected in the cornea are not observed (compare **C** and **F**). **D,E,F** adapted from (Shi et al., 2009).

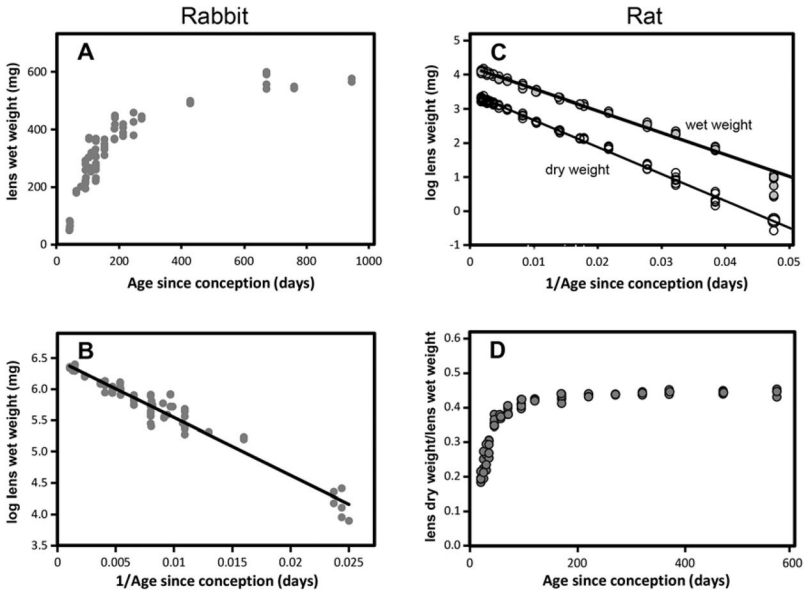

Figure 10.

Microspherophakia in a Weill-Marchesani syndrome patient. Note that the borders of the lens are visible through the dilated pupil. From (Morales et al., 2009).

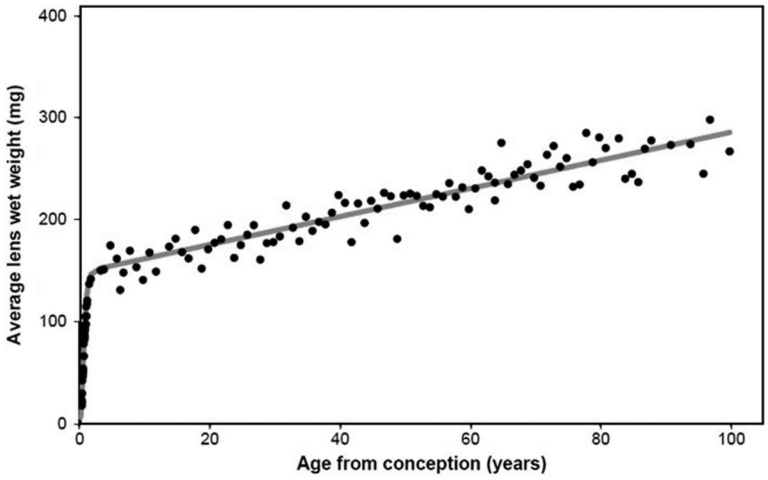

Figure 11.

The distribution of S-phase cells on the anterior lens surface can be used to define four proliferation zones. **A**. EdU-labeling index as a function of distance from the lens equator in a one-month-old mouse. **B**. Four proliferative zones (colors correspond to those shown in A) are defined: a transition zone (TZ, yellow) with little or no cell proliferation, a germinative zone (GZ, red) with high levels of proliferation, a pre-germinative zone (PGZ, blue) with moderate levels of proliferation, and a central zone (CZ, green) with little or no proliferation.

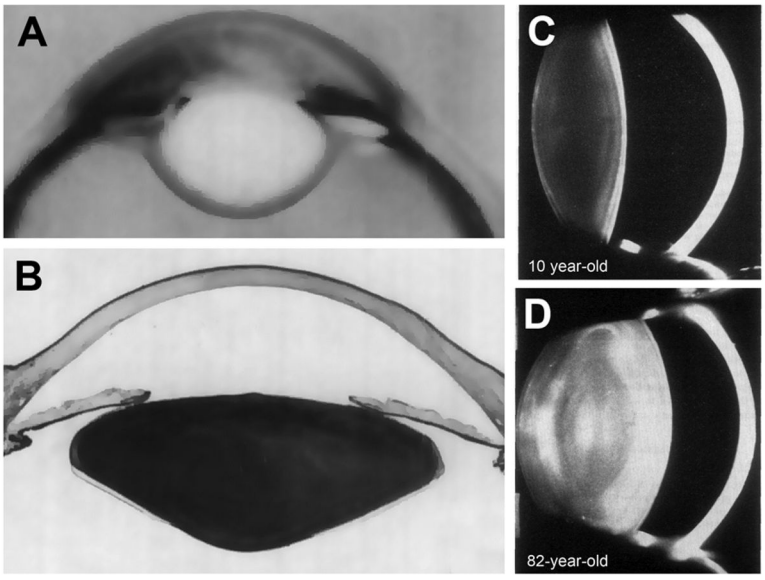

Figure 12.

Model simulation of the daily rate of fiber cell production in the mouse lens. The rate falls from about 15,000 fibers per day in the embryonic lens to a few hundred cells per day in the adult. Note the stochastic fluctuations in the rate of fiber cell production (inset). Adapted from (Sikic et al., 2017)

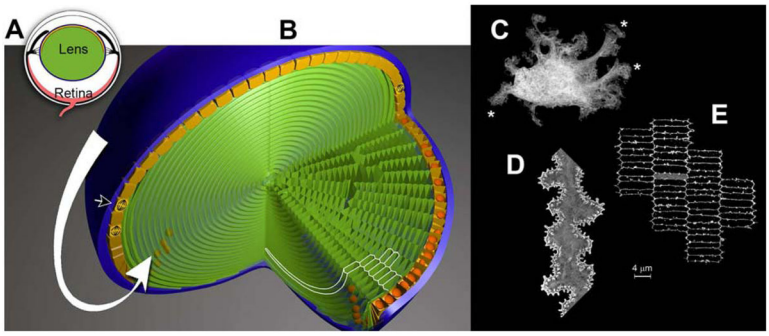

Figure 13.

Age-dependent variations in the population of the mouse lens epithelium. Colored lines represent five consecutive model simulations (all simulations commence at t=0; at early time points the simulation data are superimposable) and circles represent empirical population counts. The epithelial population increases sharply during early postnatal development, briefly exceeding 50,000 cells before declining to a lower but stable population size (≈ 43,000 cells). Model simulations capture the overshoot. Note the close agreement between sequential model runs. Adapted from (Sikic et al., 2017).

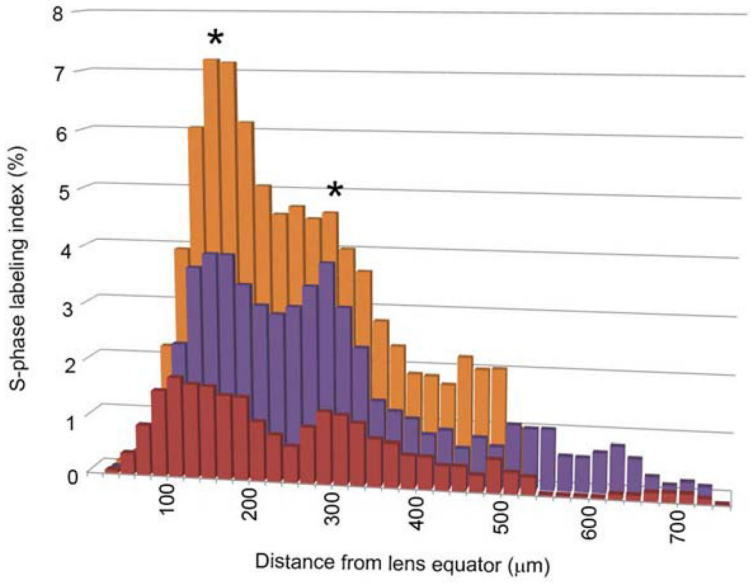

Figure 14.

Variations in zonal populations and rates of immigration/emigration in the mouse lens epithelium calculated using a stochastic lens growth model. The simulations cover the 60 day period between one and three months of age and show the number of cells (X) in each of four zones (CZ, PGZ, GZ and TZ, see Figure 11), as a function of time (in days). The daily number of cells moving between the various zones (for example, $X_{\mathrm{PGZ}\rightarrow\mathrm{CZ}}(t)$) is also indicated. The total cell population in the epithelium declines over this period (see Figure 13). This is reflected in the decrease in the population of PGZ, GZ and TZ (but not CZ, which shows a modest increase in population in response to immigration from the PGZ). The stochastic nature of the underlying growth process is evident in the fluctuating number of cells crossing the borders daily. Several hundred cells emigrate from the PGZ to the GZ per day but the main growth engine of the lens is the GZ, which supplies

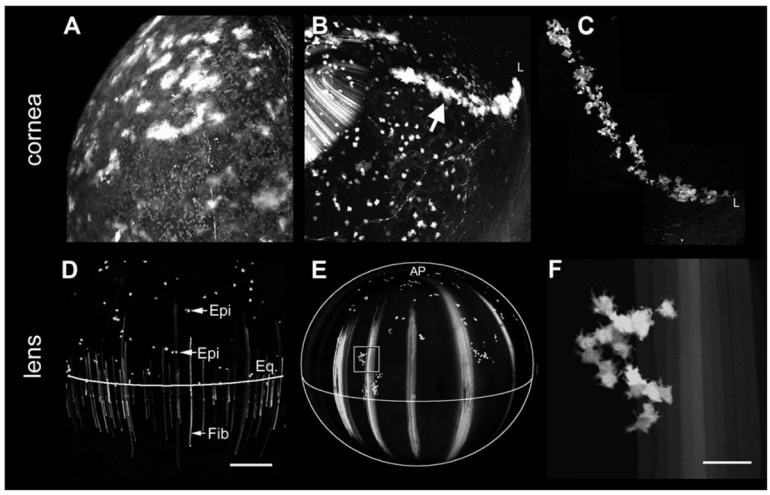

Figure 15.

Model-derived estimates of fiber cell accumulation and associated radial growth rates in the mouse lens. **A**. The fiber cell population increases rapidly during embryonic and early postnatal development but more slowly at later time points. **B**. Model simulations of radial growth (blue) are close to empirical measurements at early time points but overestimate growth at later time points. Data were corrected using linear compaction factors (see text). Model day 0 corresponds to E14.5. Figure adapted from (Sikic et al., 2017)